2011

Battery Management System For Electric Vehicle Applications

Rui Hu
University of Windsor

Battery Management System

For Electric Vehicle Applications

by

Rui Hu

A Thesis
Submitted to the Faculty of Graduate Studies
through
the Department of Electrical and Computer Engineering

in Partial Fulfillment of the Requirements for
the Degree of Master of Applied Science at the
University of Windsor

Windsor, Ontario, Canada

2011

Your file Votre référence
ISBN: 978-0-494-76296-7

Our file Notre référence
ISBN: 978-0-494-76296-7

Battery Management System

For Electric Vehicle Applications

by

Rui Hu

APPROVED BY:

_____

Dr. Randy Bowers, Outside Department Reader
Department of Mechanical, Automotive & Materials Engineering

_____

Dr. Chunhong Chen, Departmental Reader
Department of Electrical & Computer Engineering

_____

Dr. Biao Zhou, Advisor
Department of Mechanical, Automotive & Materials Engineering
Department of Electrical & Computer Engineering

_____

Dr. Mohammed Khalid, Chair of Defense
Department of Electrical & Computer Engineering

September 16th, 2011

DECLARATION OF ORIGINALITY

I hereby certify that I am the sole author of this thesis and that no part of this thesis has been published or submitted for publication.

I certify that, to the best of my knowledge, my thesis does not infringe upon anyone's copyright nor violate any proprietary rights and that any ideas, techniques, quotations, or any other material from the work of other people included in my thesis, published or otherwise, are fully acknowledged in accordance with the standard referencing practices. Furthermore, to the extent that I have included copyrighted material that surpasses the bounds of fair dealing within the meaning of the Canada Copyright Act, I certify that I have obtained a written permission from the copyright owner(s) to include such material(s) in my thesis and have included copies of such copyright clearances to my appendix.

I declare that this is a true copy of my thesis, including any final revisions, as approved by my thesis committee and the Graduate Studies office, and that this thesis has not been submitted for a higher degree to any other University or Institution.

ABSTRACT

The use of green energy is becoming increasingly more important in today's world. Therefore, electric vehicles are currently the best choice for the environment in terms of public and personal transportation. Because of its high energy and current density, lithium-ion batteries are widely used in electric vehicles. Unfortunately, lithium-ion batteries can be dangerous if they are not operated within their Safety Operation Area (SOA). Therefore, a battery management system (BMS) must be used in every lithium-ion battery, especially for those used in electric vehicles.

In this work, the purpose, functions and topologies of BMS are discussed in detail. In addition, early battery models along with the hardware and system designs for BMS are covered in a literature review. Then, an improved battery model is introduced, and simulation results are shown to verify the model's performance. Finally, the design of a novel BMS hardware system and its experimental results are discussed. The possible improvements for the battery models and BMS hardware are given in the section on conclusions and future work.

DEDICATION

To my parent!

To my wife!

To my uncle!

To ones love me!

ACKNOWLEDGEMENTS

I would like to express my deepest gratitude to my supervisors, Dr. Biao Zhou, for the guidance provided throughout the course of my research, his constructive criticism, many valuable suggestions and continuous support.

My thanks also go to Dr. Randy Bowers and Dr. Chunhong Chen for all their help and support to develop this thesis.

I specially thank all the members and previous members of the Dr. Zhou's laboratory with whom I had numerous fruitful discussions, in particular Zhi Shang.

I specially thank those who provided kindly and effective help among faculty, staff, and students at the University of Windsor.

Finally, I take the opportunity to thank my parents Aihong Zuo and Ningsheng Hu for all their love and support. I would not have been able to complete this work without their sustained encouragement.

TABLE OF CONTENTS

LIST OF TABLES

LIST OF FIGURES

1 INTRODUCTION

1.1 ELECTRICAL VEHICLE

According to previous research [1], 18% of the suspended particulates, 27% of the volatile organic compounds, 28% of Pb, 32% of nitrogen oxides, and 62% of the CO of air-borne pollution in America are produced by vehicles with internal combustion engines. In addition, 25% of energy-related CO_2 (the principle cause for the greenhouse effect) of all the CO_2 in the atmosphere are released from traditional vehicles. As an increasing number of people use public and personal transportation, the amount of air pollution increases every single day. Consequently, electric vehicles are becoming more and more popular.

An electric vehicle generally contains the following major components: an electric motor, a motor controller, a traction battery, a battery management system, a plug-in charger that can be operated separately from the vehicle, a wiring system, a regenerative braking system, a vehicle body and a frame. The battery management system is one of the most important components, especially when using lithium-ion batteries.

Currently, three types of traction batteries are available: the lead-acid, nickel-metal hydride and lithium-ion batteries. Lithium-ion batteries have a number of advantages over the other two types of batteries, and they perform well if they are operated using an effective battery management system.

1.2 LITHIUM-ION BATTERY

Lithium is the lightest metal with the greatest electrochemical potential and the largest energy density per weight of all metals found in nature. Using lithium as the anode, rechargeable batteries could provide high voltage, excellent capacity and a remarkably high-energy density.

However, lithium is inherently unstable, especially during charging. Therefore, lithium ions have replaced lithium metals in many applications because they are safer than lithium metals with only slightly lower energy density. Nevertheless, certain precautions should be made during charging and discharging. The Sony Corporation was the first company to commercialize the lithium-ion battery in 1991, which has since become popular and remains the best choice for rechargeable batteries.

The lithium-ion battery requires almost no maintenance during its lifecycle, which is an advantage that other batteries do not have. No scheduled cycling is required, and there is no memory effect in the battery. Furthermore, the lithium-ion battery is well suited for electric vehicles because its self-discharge rate is less than half of the discharge rate of lead-acid and NiMH batteries.

Despite the advantages of lithium-ion batteries, they also have certain drawbacks. Lithium ions are brittle. To maintain the safe operation of these batteries, they require a protective device to be built into each pack. This device, also referred to as the battery management system (BMS), limits the peak voltage of each cell during charging and prevents the cell voltage from dropping below a threshold during discharging. The BMS

also controls the maximum charging and discharging currents and monitors the cell temperature.

1.3 LITHIUM BATTERY CHALLENGES

The operating temperature and voltage are the most important parameters that determine the performance of lithium-ion cells [2]. Figure 1-1 and 1-2 shows that the cell operating voltage, current and temperature must be maintained within the area indicated by the green box labeled “Safe Operation Area” (SOA) at all times. The cell could be permanently damaged if it is operated outside the safety zone.

The batteries could be charged above its rated voltage or be discharged under the recommended voltage.

If the recommended upper limit of 4.2 V was exceeded during charging, excessive current would flow and result in lithium plating and overheating.

On the other hand, overly discharging the cells or storing the cells for extended periods of time would cause the cell voltage to fall below its lower limit, typically 2.5 V. This could progressively break down the electrode.

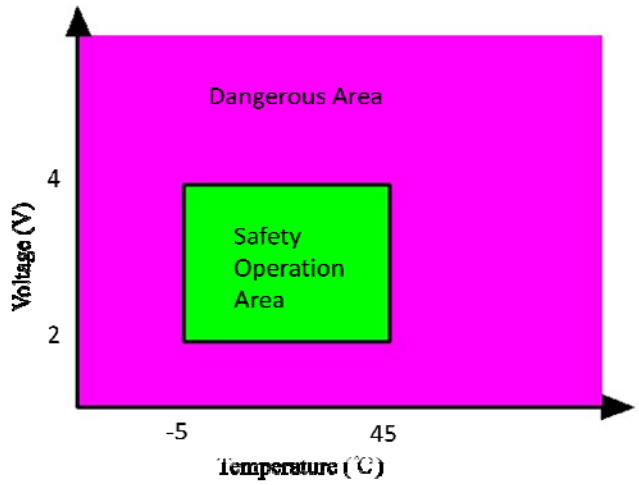

Figure 1-1 Lithium-ion cell operation window (Voltage)

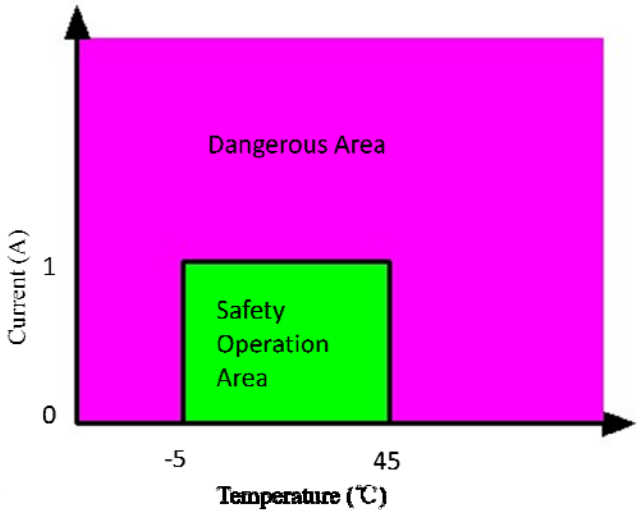

Figure 1-2 Lithium-ion cell operation window (Current)

The operating temperature of lithium-ion cells should be carefully controlled because excessively high or low temperatures could damage the cell. Temperature-related damages could be grouped into three types: low-temperature operational impact, high-temperature operational impact and thermal runaway.

While the effects of voltage and temperature on cell failures are immediately apparent, their effects on the lifecycle of the cells are not as obvious. However, the cumulative effects of these digressions may affect the lifetime of the cells.

Figure 1-3 shows that the lifecycles of the cell would be reduced if its operating temperature falls below approximately 10 °C. Similarly, their lifecycles would be reduced if the cells were operated above 40 °C. Furthermore, thermal runaway would occur when the temperature reached 60 °C. The thermal management system, which is part of the BMS, must be designed to keep the cells operating within its limitation at all times.

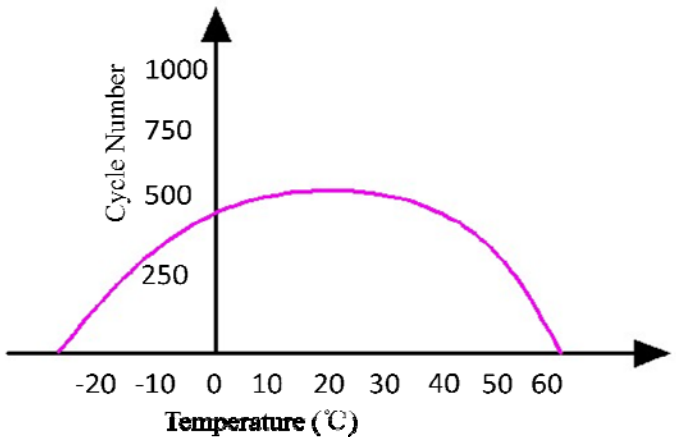

Figure 1-3 Lifecycle versus operating temperature of Li-ion cells

It is clear from the discussion above that the goal of the BMS is to keep the cells operating within their safety zone; this could be achieved using safety devices such as protection circuits and thermal management systems.

1.4 BATTERY MANAGEMENT SYSTEMS (BMS)

There are different types of BMSs that are used to avoid battery failures. The most common type is a battery monitoring system that records the key operational parameters such as voltage, current and the internal temperature of the battery along with the ambient temperature during charging and discharging. The system provides inputs to the protection devices so that the monitoring circuits could generate alarms and even disconnect the battery from the load or charger if any of the parameters exceed the values set by the safety zone.

The battery is the only power source in pure electric vehicles. Therefore, the BMS in this type of application should include battery monitoring and protection systems, a system that keeps the battery ready to deliver full power when necessary and a system that can extend the life of the battery. The BMS should include systems that control the charging regime and those that manage thermal issues.

In a vehicle, the BMS is part of a complex and fast-acting power management system. In addition, it must interface with other on-board systems such as the motor controller, the climate controller, the communications bus, the safety system and the vehicle controller.

1.4.1 DEFINITION OF THE BMS

While the definition of a BMS could differ depending on the application, the basic task of the BMS could be defined in the following manner, according to [3]:

- It should ensure that the energy of the battery is optimized to power the product;
- It should ensure that the risk of damaging the battery is minimal;
- It should monitor and control the charging and discharging process of the battery.

1.4.2 OBJECTIVES OF THE BMS

According to the definition, the basic tasks of the BMS are identical to its objectives. Although different types of BMS have different objectives, the typical BMS follows three objectives:

- It protects the battery cells from abuse and damage;
- It extends the battery life as long as possible;
- It makes sure the battery is always ready to be used.

1.4.3 FUNCTIONS OF THE BMS

1. Discharging control

The primary goal of a BMS is to keep the battery from operating out of its safety zone. The BMS must protect the cell from any eventuality during discharging. Otherwise, the cell could operate outside of its limitations.

2. Charging control

Batteries are more frequently damaged by inappropriate charging than by any other cause. Therefore, charging control is an essential feature of the BMS. For lithium-ion batteries, a 2-stage charging method called the constant current – constant voltage (CC-CV) charging method is used.

During the first charging stage (the constant current stage), the charger produces a constant current that increases the battery voltage.

When the battery voltage reaches a constant value, and the battery becomes nearly full, it enters the constant voltage (CV) stage. At this stage, the charger maintains the constant voltage as the battery current decays exponentially until the battery finishes charging.

3. State-of-Charge Determination

One feature of the BMS is to keep track of the state of charge (SOC) of the battery. The SOC could signal the user and control the charging and discharging process. There are three methods of determining SOC: through direct measurement, through coulomb counting and through the combination of the two techniques.

To measure the SOC directly, one could simply use a voltmeter because the battery voltage decreases more or less linearly during the discharging cycle of the battery.

In the coulomb-counting method, the current going into or coming out of a battery is integrated to produce the relative value of its charge. This is similar to counting the currency going into and out of a bank account to determine the relative amount in the account.

In addition, the two methods could be combined. The voltmeter could be used to monitor the battery voltage and calibrate the SOC when the actual charge approaches either end. Meanwhile, the battery current could be integrated to determine the relative charge going into and coming out of the battery.

4. State-of-Health Determination

The state of health (SOH) is a measurement that reflects the general condition of a battery and its ability to deliver the specified performance compared with a fresh battery.

Any parameter such as cell impedance or conductance that changes significantly with age could be used to indicate the SOH of the cell. In practice, the SOH could be estimated from a single measurement of either the cell impedance or the cell conductance.

5. Cell Balancing

Cell balancing is a method of compensating weaker cells by equalizing the charge on all cells in the chain to extend the overall battery life. In chains of multi-cell batteries, small differences between the cells due to production tolerances or operating conditions tend to be magnified with each charge-discharge cycle. During charging, weak cells may be overstressed and become even weaker until they eventually fail, causing the battery to fail prematurely.

To provide a dynamic solution to this problem while taking into account the age and operating conditions of the cells, the BMS may incorporate one of the three cell-balancing schemes to equalize the cells and prevent individual cells from becoming overstressed: the active balancing scheme, the passive balancing scheme and the charge shunting scheme.

In active cell balancing, the charge from the stronger cells is removed and delivered to the weaker cells.

In passive balancing, dissipative techniques are used to find the cells with the highest charge in the pack, as indicated by higher cell voltages. Then, the excess energy is removed through a bypass resistor until the voltage or charge matches the voltage on the weaker cells.

In charge shunting, the voltage on all cells would be leveled upward to the rated voltage of a good cell. Once the rated voltage of the cell is reached, the current would bypass the fully charged cells to charge the weaker cells until they reach full voltage.

6. Logbook Function

Because the SOH is relative to the condition of a new battery, the measurement system must hold a record of the initial conditions or a set of standard conditions for comparison.

An alternative method of determining the SOH is to estimate the SOH value based on the usage history of the battery rather than on certain measured parameters, such as the number of charge-discharge cycles completed by the battery. Therefore, the logbook function of the BMS would record such important data to the memory system.

7. Communications

The communications function of a BMS may be provided though a data link used to monitor performance, log data, provide diagnostics or set system parameters. The function may also be provided by a communications channel carrying system control signals.

The choice of the communications protocol is not determined by the battery; instead, it is determined by the application of the battery. The BMS used in electric vehicles must communicate with the upper vehicle controller and the motor controller to ensure the proper operation of the vehicle.

There are two major protocols used by the BMS to communicate with the vehicle: through the data bus or the controller area network (CAN) bus. Data buses include the RS232 connection and EIA-485 (also called the RS485 connection). The industry standard for on-board vehicle communications is the CAN bus, which is more commonly used in vehicle applications.

1.4.4 BMS TOPOLOGY

Three basic topologies are used in the design of BMS hardware.

1. Distributed Topology

In distributed topology, voltage monitors and discharge balancers with digital communications that can cut off the charger and report its status are placed on each cell.

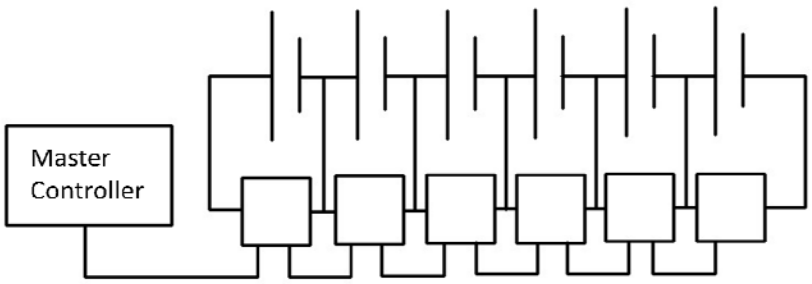

Figure 1-4 Distributed topology

The advantages of this design include its simplicity and high reliability. The disadvantages include the requirement of a large number of mini-slave printed circuit boards and the difficulty of mounting the boards on certain types of cells.

2. Modular Topology

In the modular structure, several slave controllers are used to consolidate the data to a master controller.

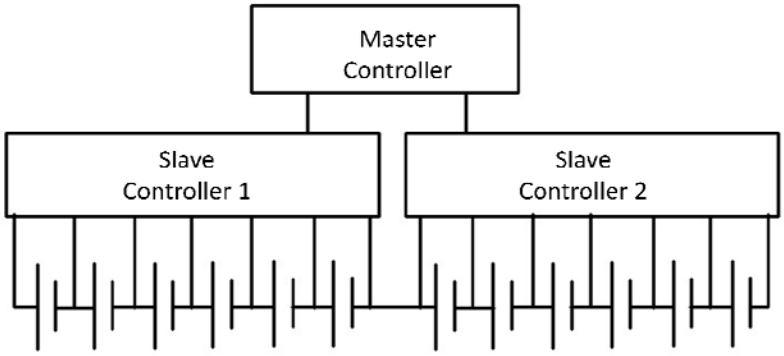

Figure 1-5 Modular topology

No printed circuit boards are necessary to connect the individual cells. However, isolated master-slave communications are difficult to achieve when this structure is used in electric vehicles.

3. Centralized Topology

In centralized topology, a centralized master control unit is directly connected to each cell of the battery pack. The control unit protects and balances all cells while providing various other functions.

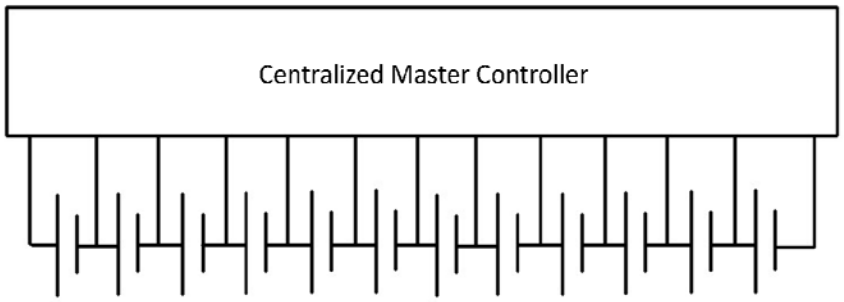

Figure 1-6 Centralized topology

Using this topology only requires a single installation point and no complex inter-vehicle communications. However, excess heat could be generated because the controller is the only source for cell balancing. In addition, the cells are distributed within various locations of the vehicle, which requires wiring to a central location.

2 LITERATURE REVIEW OF BMS

2.1 REVIEW OF BATTERY MODELING

In the automotive industry, reducing greenhouse gas emissions is the most important issue. By using electric vehicles, greenhouse gas emission could be reduced; furthermore, the electricity distribution system would also be affected. One of the central components in an electric vehicle is the battery, which stores a large amount of energy and enables functions such as regenerative braking. In addition, it releases electrical energy when necessary and supplements slow dynamic energy sources such as fuel cells. The main goal for the BMS is to ensure that the battery is always charged. To achieve this goal, a detailed simulation of the traction system in the electric vehicle and a detailed battery model is required to design the BMS.

2.1.1 SHEPHERD MODEL

Clarence M. Shepherd proposed a battery model [4] in 1965. In his work, he derived an equation that described the discharging processes of different cells by calculating the cell potential during discharge, which is a function of discharge time, current density, and other factors. Using only a small amount of experimental data, he provided a complete description of the characteristics of a discharging cell. The model described cell charges, cell capacities, and the power evolution of the cells, while simultaneously pointing out experimental errors.

However, the following assumptions were required when the model was analyzed mathematically:

(A) Porous active materials were present in the anode and/or the cathode.

(B) During discharging, the electrolyte resistance remained constant.

(C) The discharging current remained constant.

(D) The polarization was linear with the active material current density.

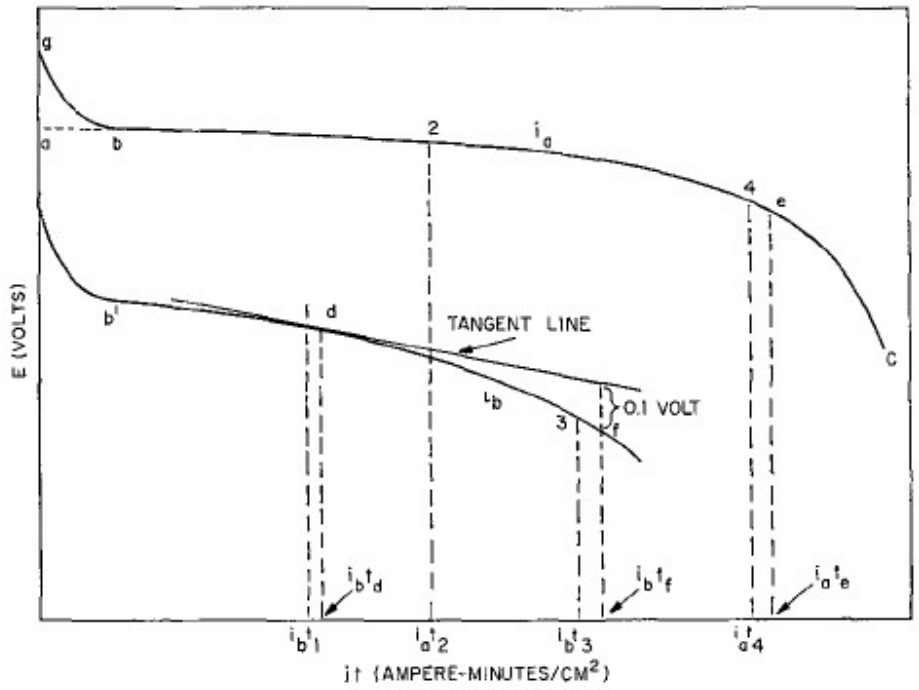

Figure 2-1 Battery Discharging Curve [4]

The two solid curves (ia and ib) shown in Figure 2-1 represent the typical battery behavior when they discharge. The potential (shown as the y-axis in volts) is plotted as a function of (it). The x-axis is the amount of electricity supplied by the battery at time t. The derivation that follows the polarization is linear to the right of point b and b', which

are assumed. If only polarization is considered, then Ec, the cathode potential during discharge, is defined as

$$E_c = E_{sc} - K_c i_{am} \quad [1]$$

where

Ec: the cathode potential (V)

Esc: the constant potential (V)

Kc: the cathode coefficient of polarization per unit active material current density (Ωcm^2)

iam: the active material current density(A/ cm^2)

Although this equation can be used as a fundamental equation in the derivation that follows, the theoretical factors associated with this equation may not apply to most discharging processes of a battery.

The current density iam in a porous active electrode is inversely proportional to the amount of unused active material. In addition, iam is equal to i at the beginning of the discharge. Therefore,

$$i_{am} = \left(\frac{Q_c}{Q_c - it} \right) i \quad [2]$$

where

t: the time at any point during the discharge (h)

Qc: the amount of available active material in the cathode expressed as ampere-hours per unit area. (Ah/cm^2)

i_{am}: the current density (A/cm^2) of the active material

i: the current density (A/cm^2)

When Eq. [2] is substituted in Eq. [1], we have

$$E_c = E_{sc} - K_c\left(\frac{Q_c}{Q_c - it}\right)i \quad [3]$$

Similarly,

$$E_a = E_{sa} - K_a\left(\frac{Q_a}{Q_a - it}\right)i \quad [4]$$

where the subscripts a and c denote anode and cathode, respectively. The value of the potential term is positive as given by the sign convention used in this work.

Generally, Qa is approximately equal to Qc in a well-designed cell. Therefore, Eq. [3] and [4] can be summed to give

$$E = E_s - K\left(\frac{Q}{Q - it}\right)i \quad [5]$$

where

E is the potential of the cell in volts (neglecting internal resistance) at any time t during the discharge; it is also equal to the sum of Ea and Ec.

Es is a constant potential in volts equal to the sum of Esa and Esc.

K is the polarization coefficient and equal to Ka plus Kc (Ωcm^2).

Q is the amount of available active material, which is equal to Qa and Qc (Ah/cm^2).

i is the current density (A/cm^2).

t is the time at any point during the discharge (h).

When Qc is not equal to Qa, the value of Q is determined by the amount of available active material on the electrode that fails first or the controlling electrode. This equation can also approximate the battery potential when several cells are connected in series to form a battery.

When the internal resistance of a battery is considered, Eq. [5] becomes

$$E = E_s - K\left(\frac{Q}{Q-it}\right)i - Ri \qquad [6]$$

where

R is the internal resistance per unit area measured in Ωcm^2.

The results from evaluating equation [6] mathematically are plotted in Figure 2-1. A dotted line is drawn from a to b, and a solid line is drawn from b to c in the figure. The initial potential drop at the beginning of the discharge was not observed in the curves drawn with the results from equation 6. Therefore, the potential calculated from equation [6] (shown as the dotted line) must be corrected by adding another term to the model to approximate the actual discharge potential (shown as the solid line from g to b). The expression $Aexp(-BQ^{-1}it)$ was found to give an excellent estimate of the initial potential drop in virtually every case, where A and B were empirical constants. Therefore, the final equation was obtained after this term was added to equation [6]:

$$E = E_s - K\left(\frac{Q}{Q-it}\right)i - Ri + A\exp(-BQ^{-1}it) \qquad [7]$$

In a number of cases, the initial potential drop was too sharp to be included in the experimental data; the expression $Aexp(-BQ^{-1}it)$ was neglected in these cases.

If the numerical values of Es, K, Q, and N were known, and the basic assumptions were true, equation [6] could be used to predict the discharge curve to the right of point b in Figure 2-1. However, discharge curves could be obtained more easily and accurately through experiments than through calculations. Nevertheless, empirical values of Es, K, Q, N, A, and B could be determined by numerically fitting equation [6] to experimental discharge data. One could then obtain an accurate description of the cell or battery discharge process that could also be used to describe energy evolution and cell capacity; it could even be used to predict cell capacities. Because the numerical values of K, Q, and N could be determined by numerical fitting, they could vary considerably from their true values as defined in the basic assumptions.

2.1.2 TREMBLAY MODEL

Olivier Tremblay presented an easy-to-use battery model using dynamic simulation software [5]. To avoid the problem of forming an algebraic loop, this model only used the SOC of the battery as a state variable. This model accurately represented battery chemistries that consisted of a controlled voltage source placed in series with an internal resistance. The parameters of the model could be extracted easily from the discharge curve given by the manufacturer for ease of use.

Three types of basic battery models are used in the literature: the experimental, electrochemical and electric circuit-based models. The experimental and electrochemical models are not suitable to represent cell dynamics and to estimate the SOC of battery

packs. However, the electric circuit-based model is useful in representing the electrical characteristics of the batteries. The simplest electric circuit-based model consists of an ideal voltage source in series with an internal resistance. Unfortunately, this model does not take the SOC of the battery into account. Therefore, Tremblay used an equation to describe the electrochemical behavior of a battery in terms of the terminal voltage, open-circuit voltage, and internal resistance. The model for the discharge current and SOC was developed by Shepherd, which was applicable to both the discharging and charging processes. However, this model causes an algebraic loop problem in the closed-loop simulation of modular models.

In the original Shepherd model, a non-linear term equal to $KQ/(Q - it)\ i$ was used to represent the non-linear voltage that changed with the amplitude of the current and the actual charge of the battery. In this model, the battery voltage increased to nearly E_0 when the battery was almost completely discharged, and no current was flowing. Then, the voltage fell abruptly as soon as the current began to circulate again. Although the behavior of this model corresponded to that of a real battery, the model contained algebraic loops and simulation instabilities that made it difficult to use.

The subsequent Tremblay model included modifications that attempted to deal with this problem. The model included a term representing the non-linear voltage that depended uniquely on the actual battery charge; the voltage became nearly 0 when the battery was almost completely discharged with no current flowing. Like the Shepherd model, this model represented the behavior of the battery and produced accurate results.

The equations used to describe the battery in the electric circuit-based model became:

$$E = E_0 - K\frac{Q}{Q - it} + A\exp(-Bit) \quad [8]$$

$$V = E - Ri \quad [9]$$

where

E = no-load voltage (V)

E_0 = battery constant voltage (V)

K = polarization voltage (V)

Q = battery capacity (Ah)

it = actual battery charge (Ah)

A = exponential zone amplitude (V)

B = exponential zone time constant inverse $(Ah)^{-1}$

V = battery voltage (V)

R = internal resistance (Ω)

i = battery current (A)

t = time (h)

The electric circuit-based model had a simple controlled voltage source in series with a constant resistance, as shown in Figure 2-2.

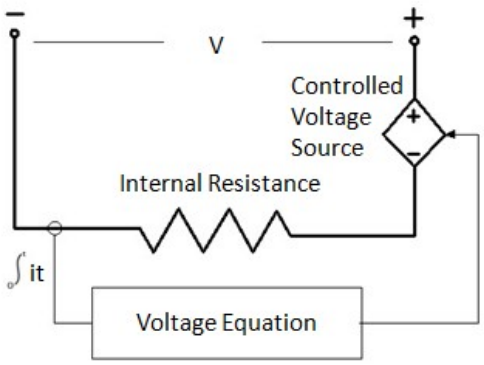

Figure 2-2 Electric circuit-based model

The open-voltage source was calculated with a non-linear equation based on the actual SOC of the battery. The model assumed the same characteristics for the charge and discharge cycles.

The SOC is given by:

$$SOC = 100\% \times (1 - \frac{\int idt}{Q}) \quad [10]$$

where

Q = battery capacity (Ah)

i = battery current (A)

t = time (h)

There were two limitations in the Tremblay model. First, the minimum no-load battery voltage was 0 V, whereas the maximum battery voltage was not limited. Second, the minimum capacity of the battery was 0 Ah, whereas the maximum capacity was not limited. Therefore, the maximum SOC can be greater than 100% if the battery is overcharged.

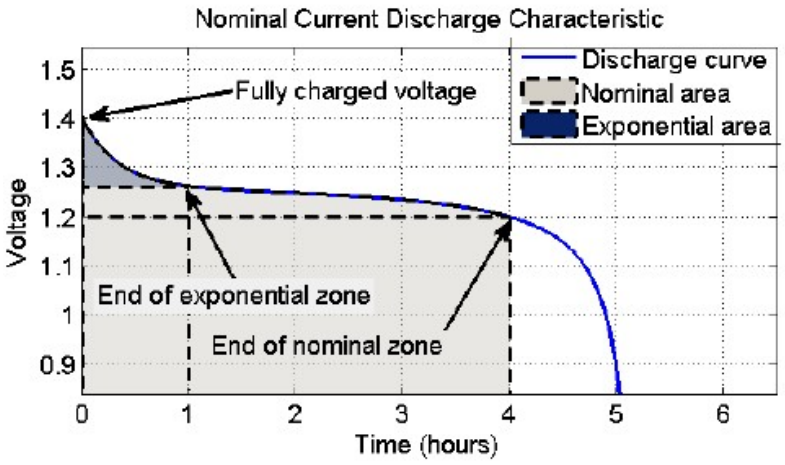

Figure 2-3 Discharge curve of a 1.2-V, 6.5-Ah cell [5]

The parameters in the Tremblay model could be easily deduced from the discharge curve provided by the manufacturers. Figure 2-3 shows the typical discharge characteristics for a 1.2-V and 6.5-Ah NiMH cell. Once the parameters were well determined, the Tremblay model could accurately represent the behavior of many types of batteries.

2.2 BMS HARDWARE REVIEW

The research on BMS hardware systems has been conducted in both the academic field and the commercial field.

2.2.1 REVIEW ON COMMERCIAL BMS

Because the concept of electric vehicles is relatively new, the BMS of electric vehicles is also under development. Commercialized BMSs, also called off-the-shelf BMSs, are only available from dozens of manufactures, and more systems may become available in the

coming years. To understand the rapidly changing market, it is important to know the price of products, the types of products and their available features.

A larger number of commercial BMSs with basic functions suitable for smaller batteries and applications, such as laptops, is offered by Chinese manufacturers. Unfortunately, they are not suitable for large lithium-ion battery packs. High-quality BMSs are available to companies from large manufacturers that are more trusted and well known; however, these products are not available to the public.

Only several practical and economically advanced BMSs are available from small European and U.S. manufacturers that are reliable and effective.

Simple analog BMSs use analog technology, and their prices range from $16 per cell for a distributed BMS to $2 per cell for a protector. Although these BMSs have limited functions, various types of analog BMSs could be used in large lithium-ion battery packs. More sophisticated digital BMSs have more functions, and they are used in electric vehicles.

2.2.2 REVIEW ON BMS RESEARCH

In low-power applications that require only simple BMSs, such as cell phones and laptops, they could be designed from integrated circuits. However, electric vehicles require numerous large battery cells that are more problematic and more costly to repair.

References [6] – [12] describe microcontroller-based battery management solutions that include mainly monitoring systems without battery protection functions. References [13] – [15] focus more on charge equalization (also called cell balancing).

A lithium-ion BMS for electric vehicles based on CAN-bus was proposed in [16]. This BMS could sample battery information, estimate the SOC of the battery and communicate with the vehicle controller. Although the BMS did not have the cell-balancing feature, it worked successfully in the electric car manufactured by Tianjin Qingyuan Electric Vehicle Inc. The design structure is shown in Figure 2-4.

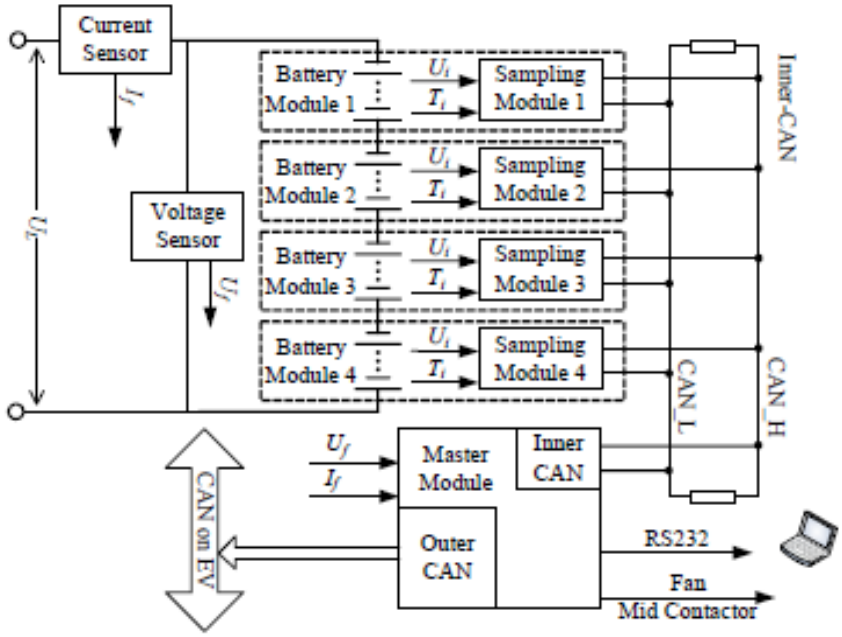

Figure 2-4 Structure of the BMS based on CAN-bus [16]

A generalized BMS was published in [17]. The main advantage of that system compared with the existing systems was that it provided a fault-tolerant capability and battery protection. It consisted of a number of smart battery modules, and each module provided

the functions of battery equalization, monitoring, and battery protection to a string of battery cells. However, the reference did not specify the application of the BMS and was likely not designed for lithium-ion batteries.

A fully digital lithium-ion battery protection and charging system based on digital signal processor (DSP) TMS320LF2407A was discussed in [18]. Figure 2-5 shows the operation principles of this design. However, the price of the DSP was much higher than the price of the microcontroller, making the total cost of the BMS prohibitively expensive.

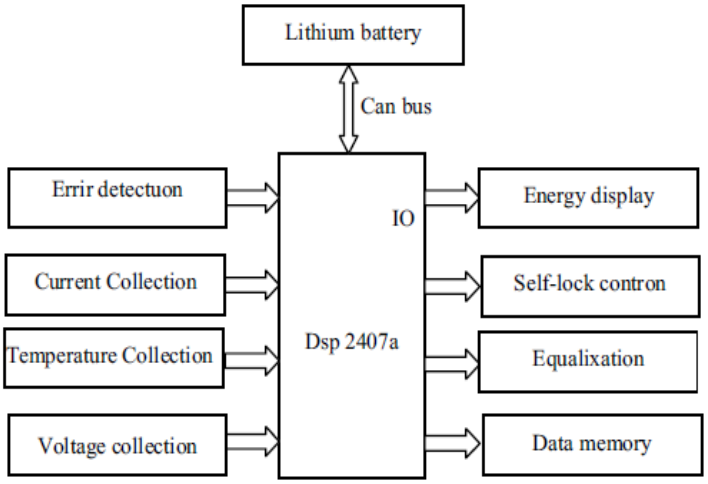

Figure 2-5 Principle of Battery Management System Based on DSP [18]

None of the previously mentioned BMS designs had a thermal management system, which is essential for electric vehicles.

2.2.3 INTRODUCTION OF THE TEXAS INSTRUMENTS BMS SYSTEM

Texas Instruments (TI) developed a BMS using digital technology and master-slave topology [19]. The company provided the front IC of the BMS, the microcontroller used in the master controller of the BMS. The programs of the BMS were programmed in C. The system included the following features: passive cell balancing, under-voltage monitoring, over-voltage monitoring, and over-temperature monitoring. It also detected whether the battery system was charging or discharging using changes in cell voltages.

2.3 SUMMARY

Battery modeling is a very complex procedure that requires a thorough knowledge of electrochemistry. However, two of the battery models mentioned above did not consider common battery behaviors, such as self-discharging and capacity fading, which made the models less accurate.

Neither of the models simulated actual battery performance because of their assumptions. These assumptions are listed below:

(1) The internal resistance was assumed constant during the charge and discharge cycles; it did not vary with the amplitude of the current.
(2) The models assumed that the parameters could be deduced from the charging and discharging characteristics.
(3) The capacity of the battery was assumed constant regardless of the amplitude of the current.
(4) The models assumed that the battery would not self-discharge.

(5) The battery was assumed to have no memory effect.

(6) The temperature was assumed to have no effect on the behavior of the model.

2.4 REARCH OBJECTIVES AND THESIS OUTLINE

Because commercial BMSs are costly and unable to meet the requirements of large electric vehicles, research on BMS hardware systems is still ongoing. It is necessary to develop an economical and fully functional BMS suitable for electric vehicles that can protect the lithium battery while prolonging its lifetime.

This thesis is divided into five chapters. Chapter 1 is the introduction of the BMS. Chapter 2 is a review of the literature on BMS. Chapter 3 introduces an improved battery model and shows the simulation results based on this model. In Chapter 4, a novel BMS hardware system design based on a BMS system by TI is introduced with several important additional functions. Experimental results are given and discussed in detail in this chapter. Chapter 5 concludes this work and suggests future work.

3 IMPROVED BATTERY MODEL

To simulate battery behaviors more accurately in the models, factors such as self-discharge, temperature, and fading capacity should be taken into consideration.

3.1 SELF-DISCHARGING EFFECT

Even without any physical connections between the electrodes, the battery can self discharge through internal chemical reactions and decreases the stored charge. This lowers the shelf life of the batteries and reduces the amount of available charge when they are put to use.

The self-discharging speed of a battery depends on the battery type, and the effect is especially strong for nickel-based rechargeable batteries. For example, nickel cadmium batteries discharge by 15 – 20% per month, whereas NiMH batteries discharge by 30% per month. Because primary batteries cannot be recharged between manufacturing and use, they have a lower self-discharge rate. Nevertheless, lithium batteries still suffer from a 2 – 3% discharge per month, which is the smallest amount of self-discharge among rechargeable batteries.

Similar to closed circuits discharge, self-discharge is a chemical reaction that occurs more quickly at high temperatures. Thus, storing batteries at low temperatures could reduce the self-discharge rate and preserve the initial energy stored in the battery.

The specific chemical causes of self-discharge depend on the particular battery, and they will not be further discussed in this work. It should be noted that self-discharge would affect battery performances in terms of SOC and cell voltage.

3.2 TEMPERATURE EFFECT

Temperature and humidity could also affect battery performances. Batteries do not operate within their normal and designed specifications when the ambient temperature exceeds the appropriate operating range. This is not a manufacturing defect but a direct consequence of extreme weather. Therefore, a battery should not be used in an environment for which it was not designed.

When the ambient temperature and relative humidity of a specific environment are altered beyond the norm, they are considered extreme weather conditions. These conditions may occur almost anywhere and at anytime. For example, extreme conditions can occur outside, in a room with no temperature control or in a closed car on a hot day. Exposing the battery to extreme weather could cause the battery to stop working and bulge, bubble, melt, become damaged, cause smoke, sparks, flames, expand, contract, or even explode in very extreme cases. Extreme weather can also occur when the relative humidity increases the ambient temperature beyond the safe operating range of the battery.

Temperature affects the operation of batteries because electrons become excited or less energized with increasing or decreasing temperature, respectively.

3.3 EFFECT OF FADING CAPACITY

It is known that lithium-ion batteries have a limited life because they gradually and irreversibly lose their capacity to hold a charge. As the battery loses its capacity, the length of time it can power a device (also called run time) decreases. As the system cycles through multiple iterations of charge and discharge, the overall performance of the battery deteriorates over time.

The typical estimated life of a lithium-ion battery is approximately two to three years or 300 to 500 charge cycles. In high-performance applications such as electric vehicles, it is important to have an accurate knowledge of the present conditions of the battery and its remaining lifetime.

3.4 IMPROVE BATTERY MODEL

Because the operation of rechargeable batteries depends on factors such as temperature, the self-discharge rate and its capacity, it is necessary to carefully develop models that accurately describe the charging and discharging behavior of batteries.

Self-discharging

The self-discharging behavior of the battery can be easily represented by adding a large resistance in parallel with the battery terminals. Figure 3-1 shows the electrical circuit that considers self-discharging. The value of the self-discharging resistance is determined by the self-discharging time of the specific battery type found in the battery data sheet.

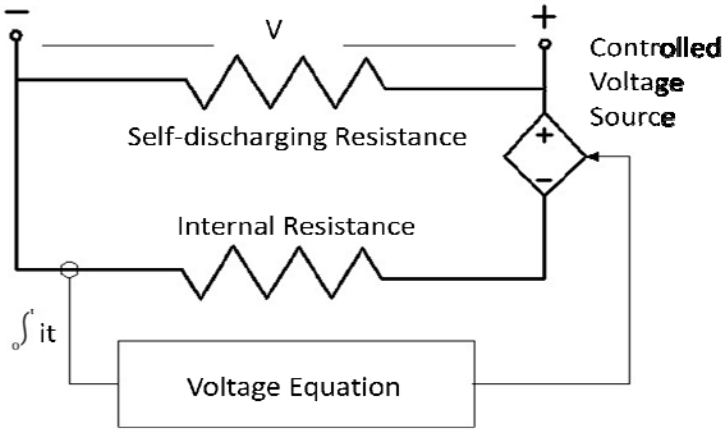

Figure 3-1 A battery model accounting for the self-discharging behavior of batteries

Then, the open circuit voltage equation becomes

$$V = E - (R + R_T)i \qquad [11]$$

where

E = no-load voltage (V)

V = battery voltage (V)

R = internal resistance (Ω)

R_T = self-discharging resistance (Ω)

i = battery current (A)

Temperature effect

To simulate the temperature effect, the term E(T) is added to Tremblay's model shown in equation [8]. The term is used to compensate for the fluctuation of the equilibrium potential induced by temperature changes. The term E(T) is equal to K_tT, where K_t is the coefficient of temperature and T is temperature.

Subsequently, the potential equation becomes

$$E = E_0 - K\frac{Q}{Q-it} + A\exp(-Bit) - K_T T \quad . \qquad [12]$$

Capacity fading

Capacity fading refers to the irreversible loss in the usable capacity of a battery due to the number of charging-discharging cycles. The term Rcycle, which changes linearly with the number of cycles, is added to the potential equation to simulate this phenomenon. The term E(C), which is equal to KcC, is added to the potential equation to represent the capacity fading effect. Finally, the potential equation and the open circuit equation can be generalized as:

$$E = E_0 - K\frac{Q}{Q-it} + A\exp(-Bit) - K_T T - K_C C \qquad [13]$$

$$V = E - (R + R_C + R_T)i \qquad [14]$$

where

K_c = the coefficient of the number of cycles

C = the number of cycles

Rc= aging resistance

3.5 SIMULATION RESULTS AND DISCUSSION

All simulations were based on the cell parameters shown in Table 3-1.

Table 3-1 Cell parameters for battery LP372548

Battery Type	LP372548
Nominal Capacity	420 mAh (0.2 C discharge)
Nominal Voltage	3.7 V (0.2 C discharge)
Charging Voltage	4.2 ± 0.05 V
Standard Charge	Method: CC/CV (constant current / constant voltage) Current: 0.5 C Voltage: 4.2 V End Current: 0.02 C
Maximum Charge Current	400 mA
Maximum Discharge Current	800 mA
End of Discharge Voltage	2.75 V
Operating Temperature	Charge: 0 ℃ ~ 45℃ Discharge: -20 ℃ ~ 60℃
Storage Temperature	-20℃ ~ 45℃ (for less than 1 month) -20℃ ~ 35℃ (for less than 6 months)

Uncontrolled charging with constant current only

As shown in the figure below, the battery voltage exceeded the high voltage limit (4.2 V) when the battery was charged using a constant current power source, which was harmful for the battery.

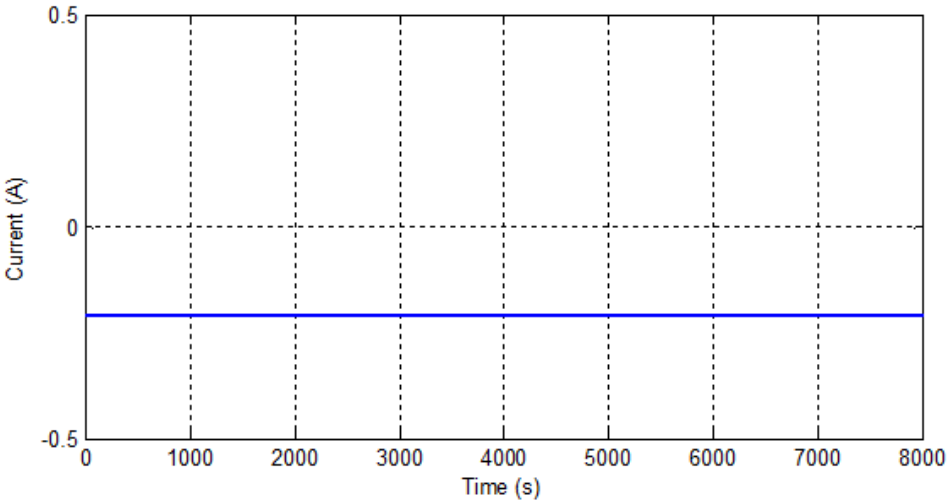

Figure 3-2 Constant Current Charging (Current)

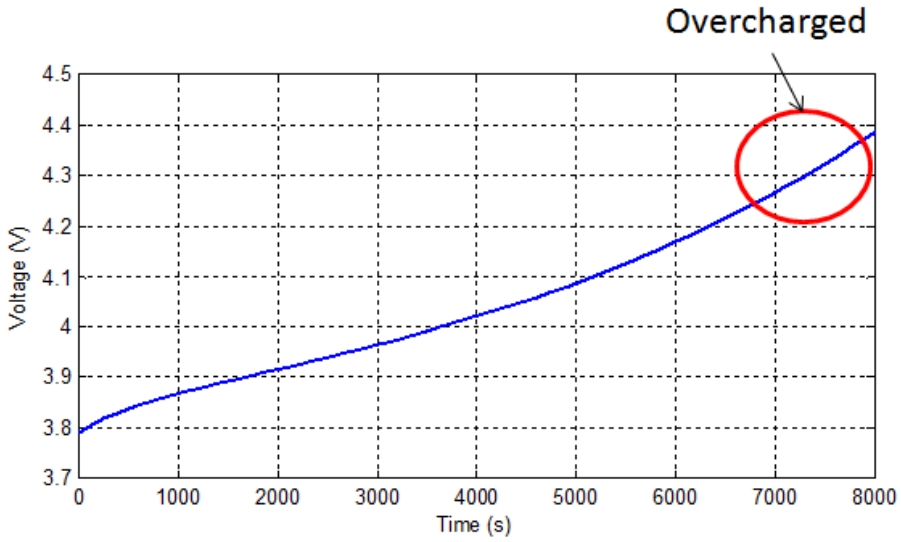

Figure 3-3 Constant Current Charging (Voltage)

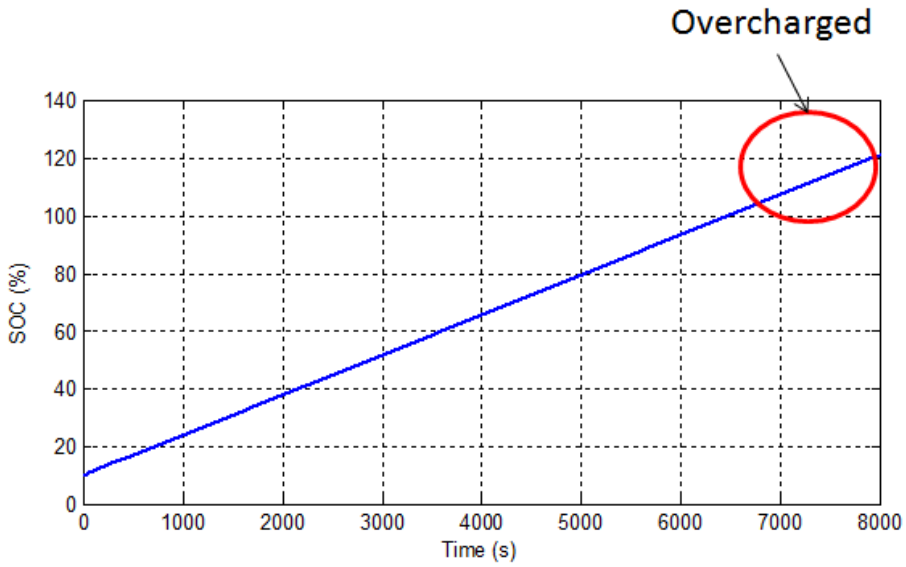

Figure 3-4 Constant Current Charging (SOC)

Uncontrolled charging with constant voltage only

As shown in the figure below, the battery current exceeded the high current limit (0.21 A) when the battery was charged using a constant voltage power source. This was also harmful for the battery.

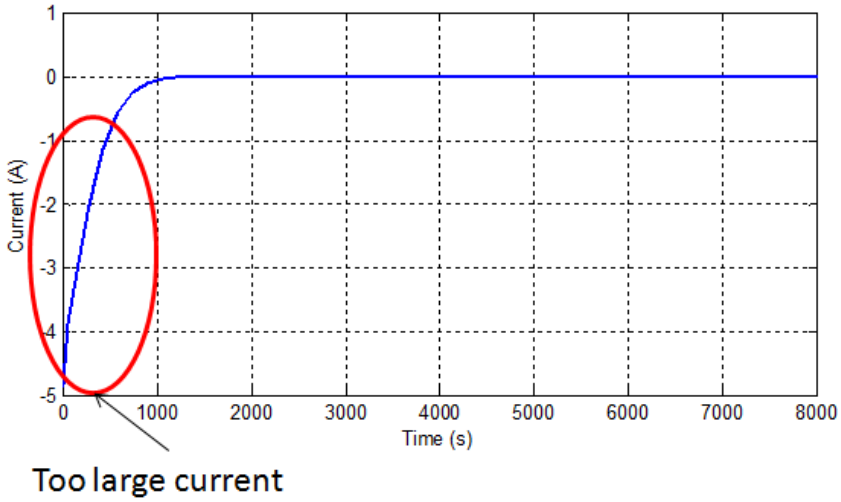

Figure 3-5 Constant Voltage Charging (Current)

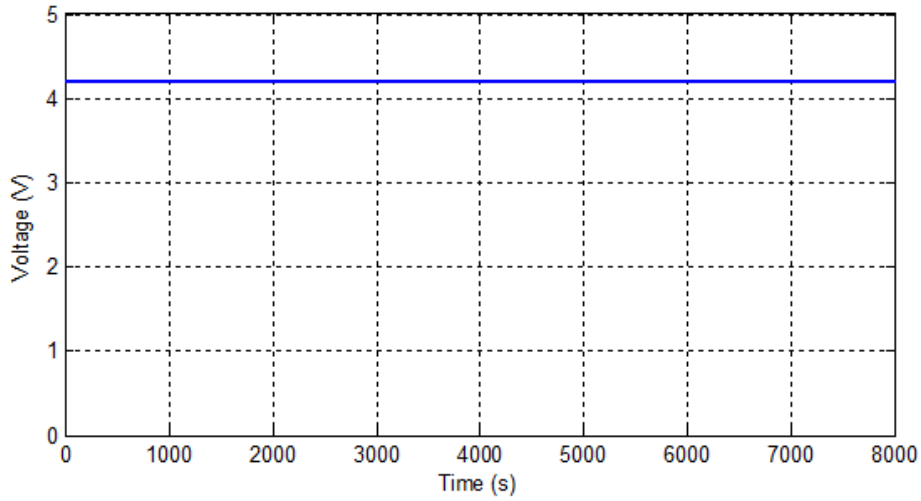

Figure 3-6 Constant Voltage Charging (Voltage)

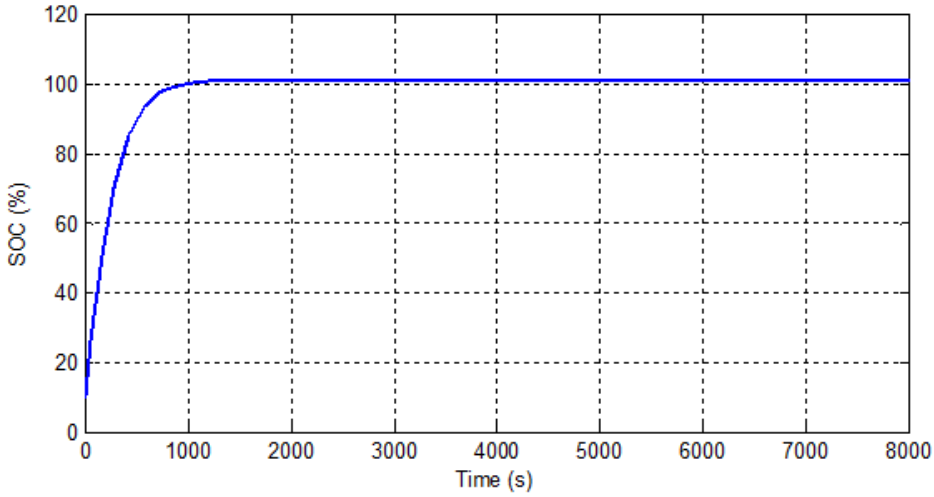

Figure 3-7 Constant Voltage Charging (SOC)

Controlled charging with CC/CV

As shown in the figure below, both the battery current and voltage remained in the SOA when the battery was charged using the CC/CV method. This was the optimal method to charge the battery.

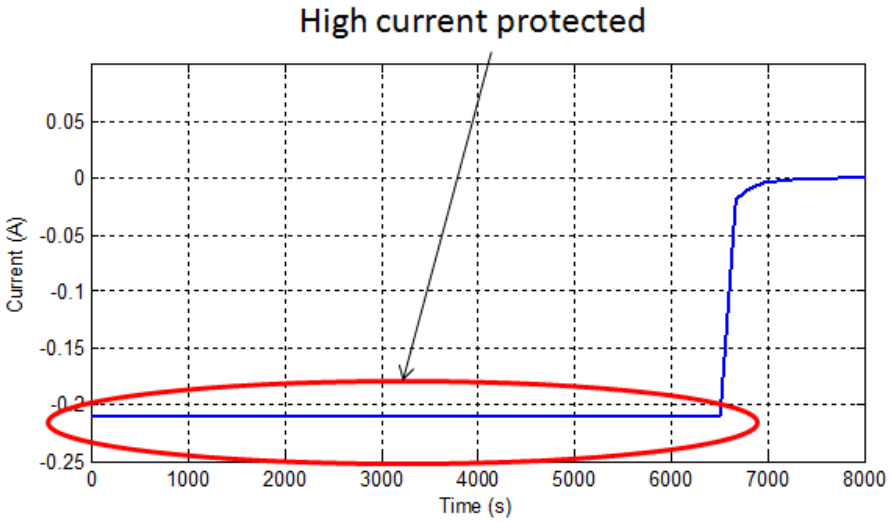

Figure 3-8 Charging with CC/CV (Current)

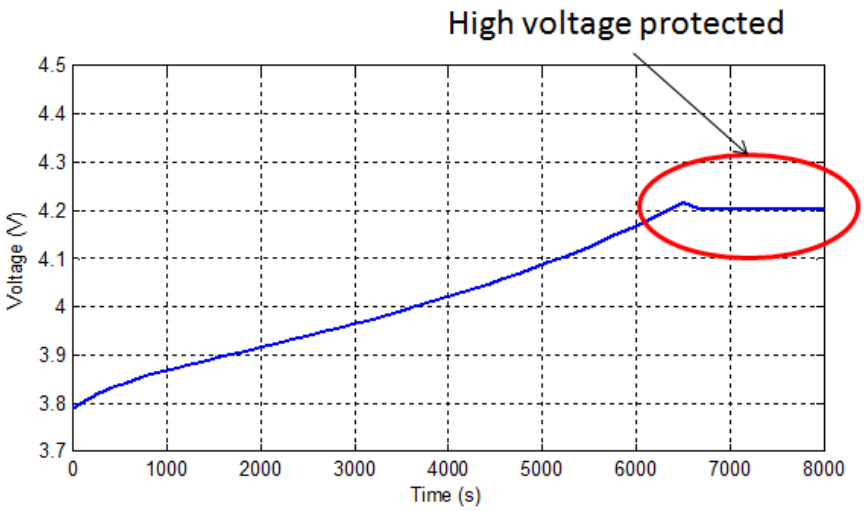

Figure 3-9 Charging with CC/CV (Voltage)

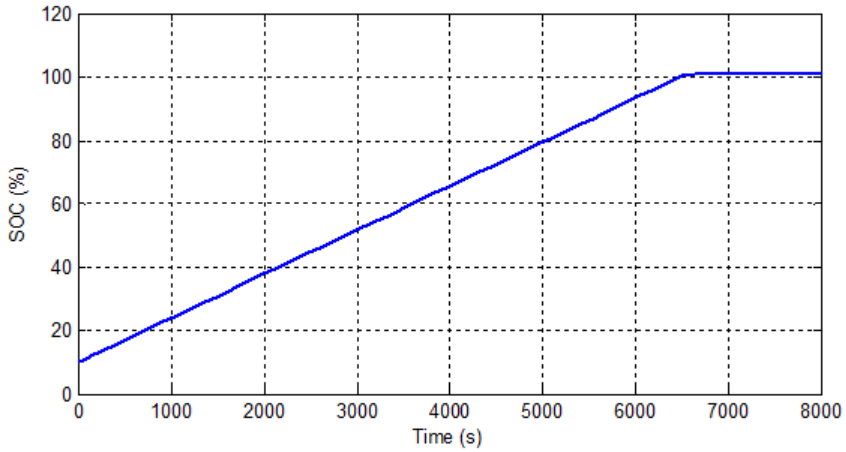

Figure 3-10 Charging with CC/CV (SOC)

Uncontrolled discharging

As shown in the figure below, the battery voltage dropped below the low voltage limit (2.75 V) when the battery was discharged without protection. This was harmful for the battery.

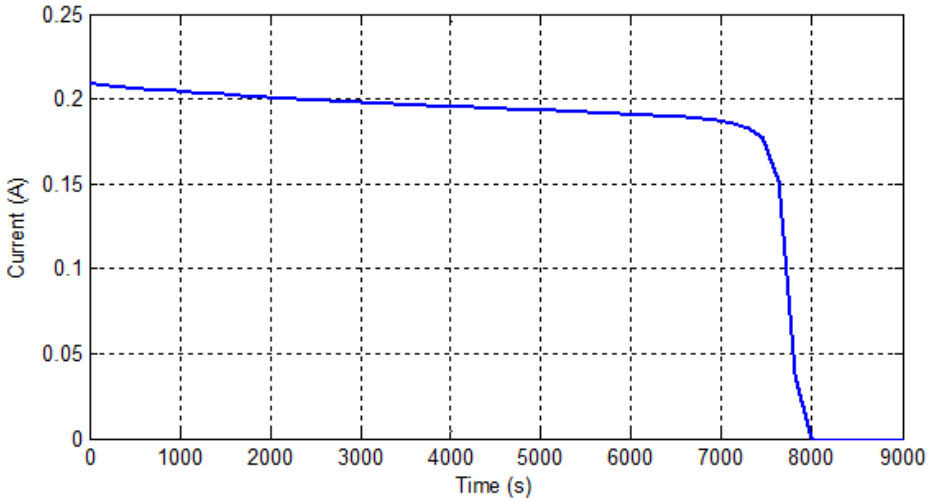

Figure 3-11 Discharging with No Protection (Current)

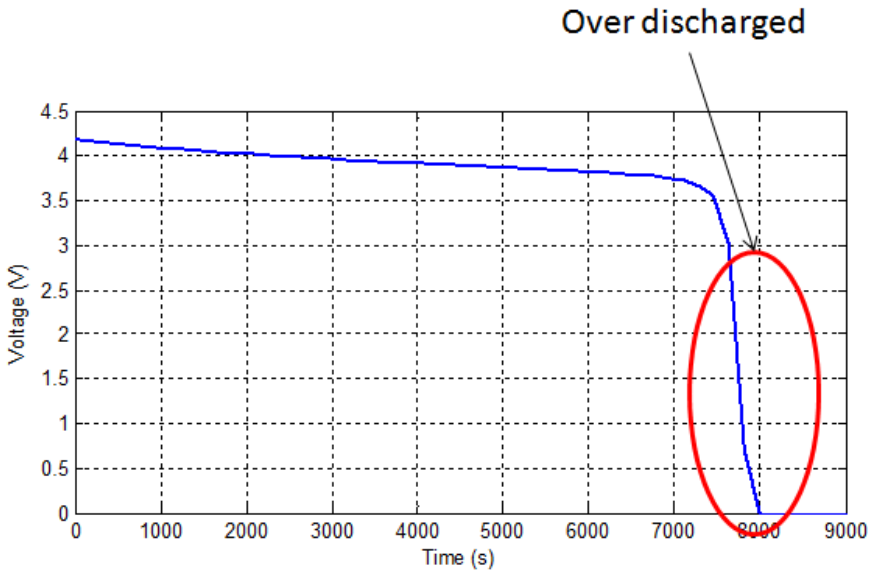

Figure 3-12 Discharging with No Protection (Voltage)

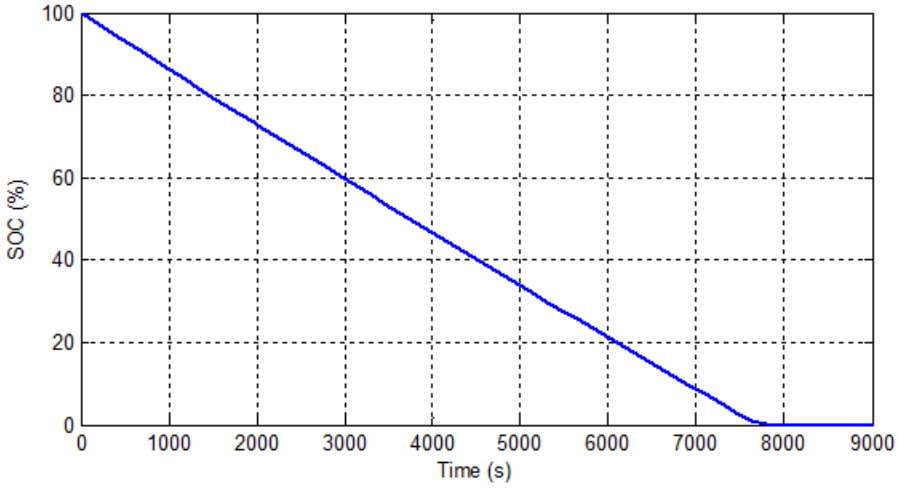

Figure 3-13 Discharging with No Protection (SOC)

Discharging with voltage protection

As shown in the figure below, the battery stopped discharging and remained at the low voltage limit (2.75 V) when the battery was discharged with voltage protection. The cell was protected by discharging in this manner.

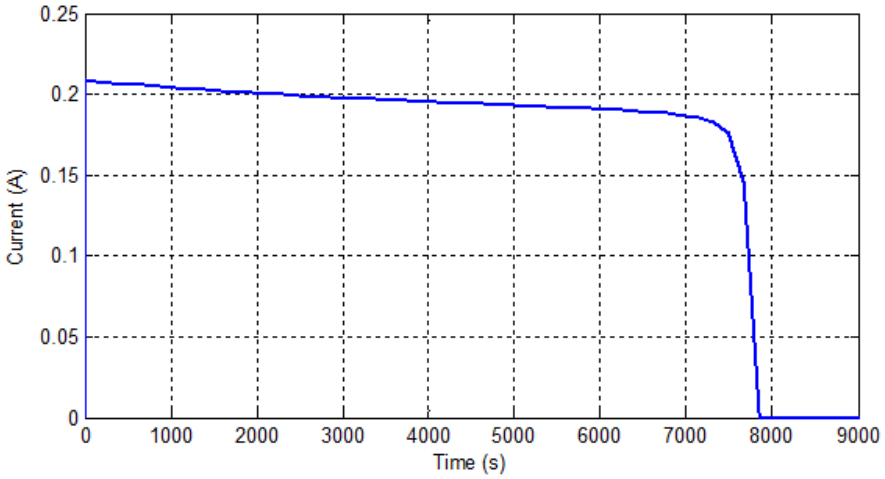

Figure 3-14 Discharging with Voltage Protection (Current)

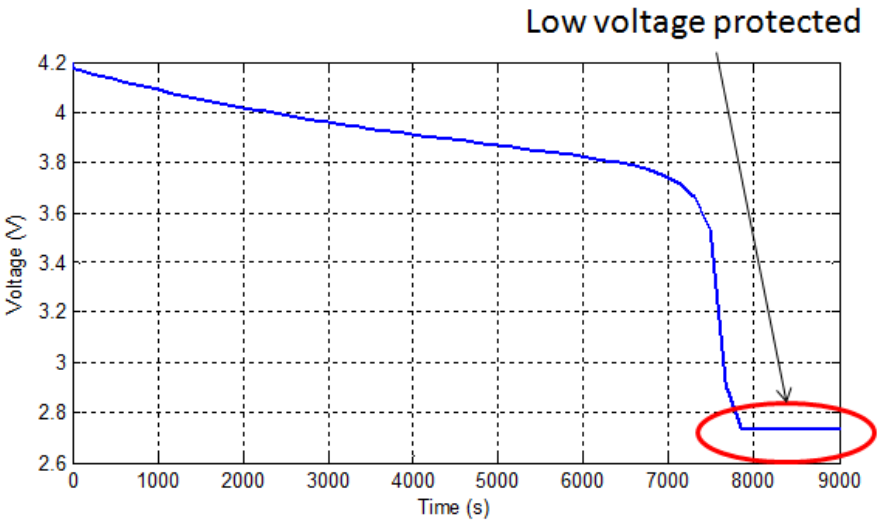

Figure 3-15 Discharging with Voltage Protection (Voltage)

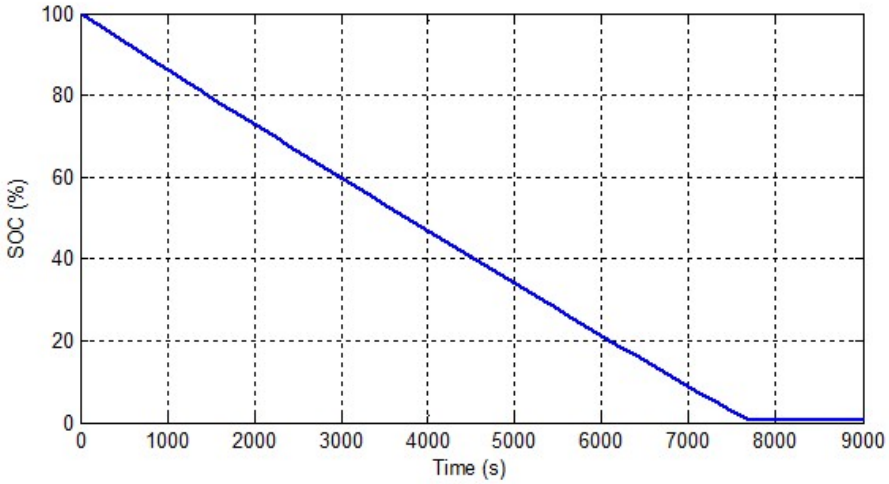

Figure 3-16 Discharging with Voltage Protection (SOC)

Discharging with current protection

As shown in the figure below, the battery was discharged at a maximum discharging current of 0.8A when it was discharged with current protection. The cell was protected by discharging in this manner.

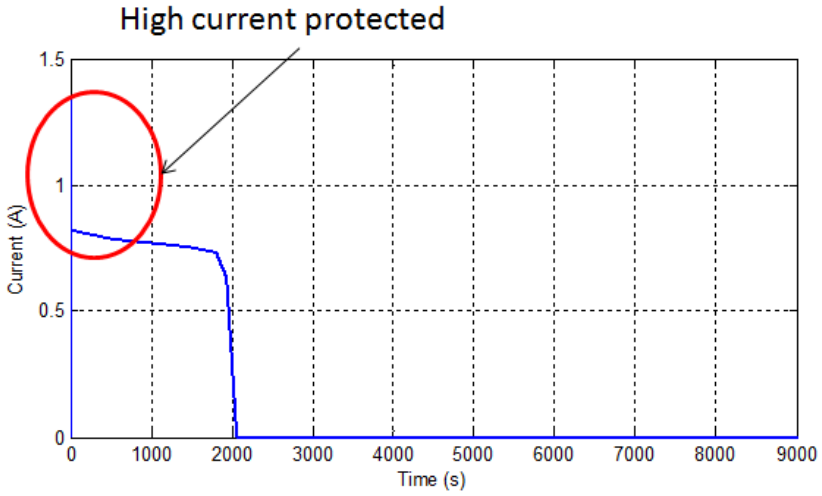

Figure 3-17 Discharging with Current Protection (Current)

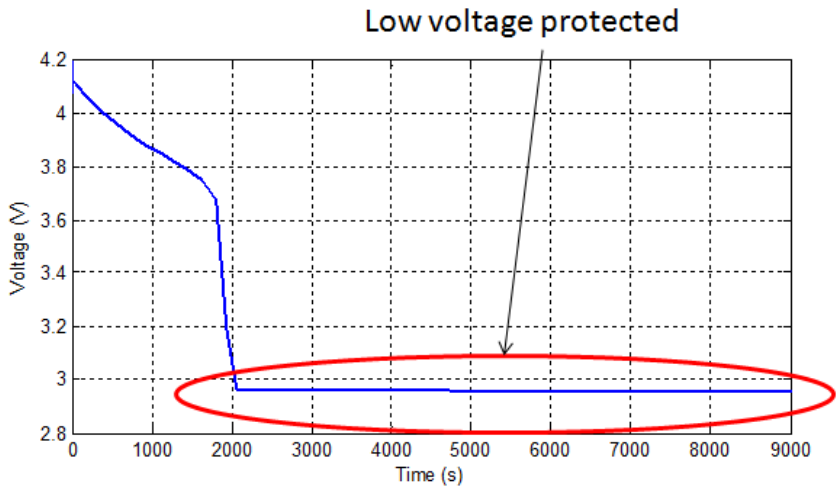

Figure 3-18 Discharging with Current Protection (Voltage)

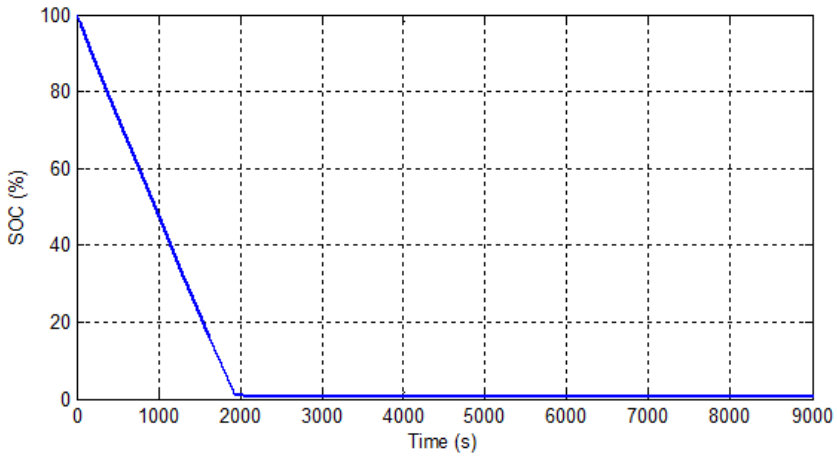

Figure 3-19 Discharging with Current Protection (SOC)

Cell-balancing simulation results

In this simulation, there were 4 cells in the battery pack and each had a different SOC. When cell balancing was active, the cells with higher capacities would discharge until they reached the lowest SOC of the cell in the battery pack to balance the entire pack.

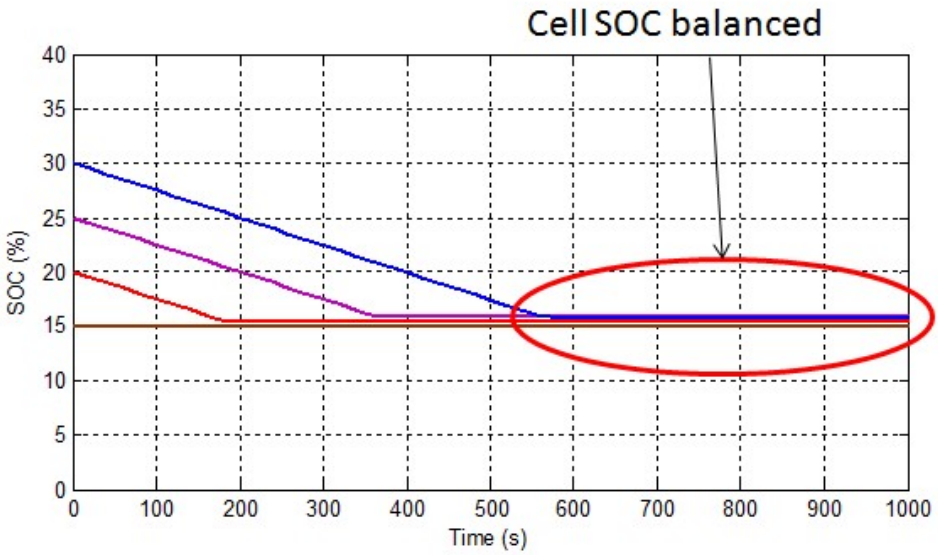

Figure 3-20 Cell-balancing results

The storage characteristics of the battery at normal temperatures

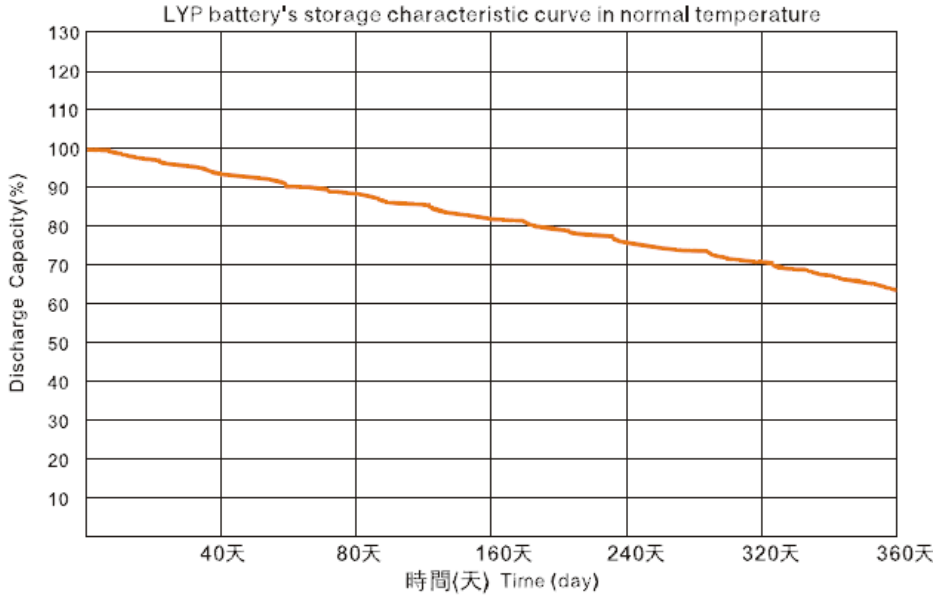

Figure 3-21 The actual self-discharging curve of the battery

Simulated storage characteristics of the battery at normal temperatures

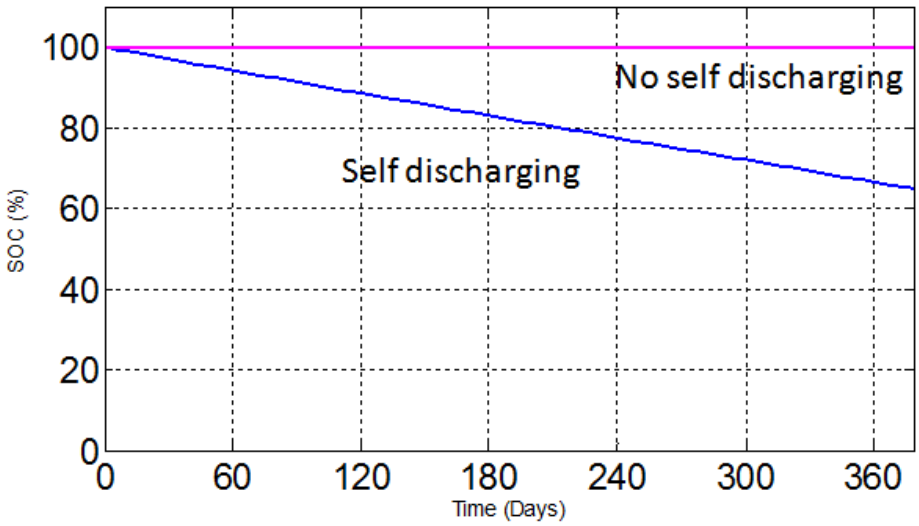

Figure 3-22 Simulated self-discharging curve of the battery model

Simulated discharge curves of the battery under different temperatures

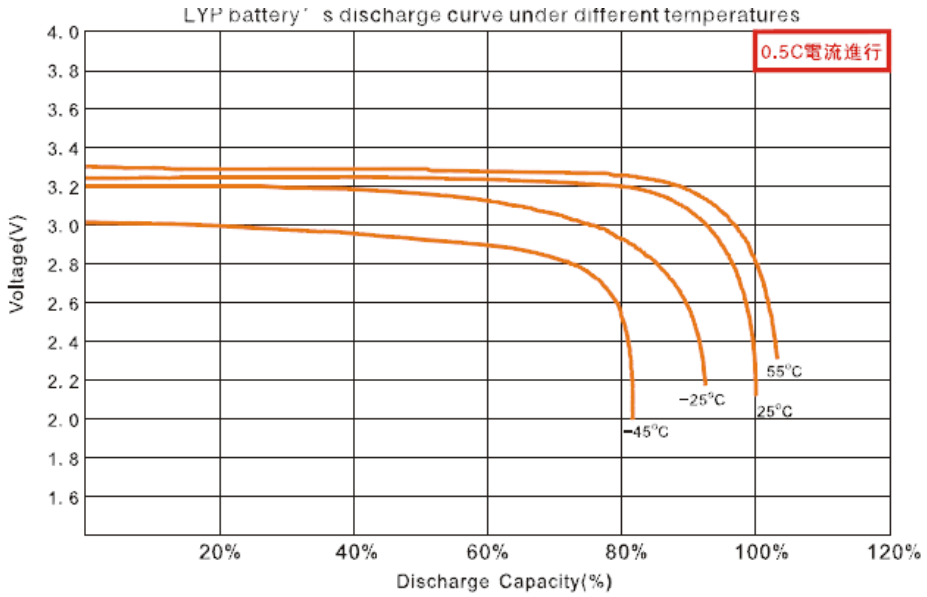

Figure 3-23 The actual discharging curve of the battery under different temperatures

Simulated discharge curves of the battery under different temperatures

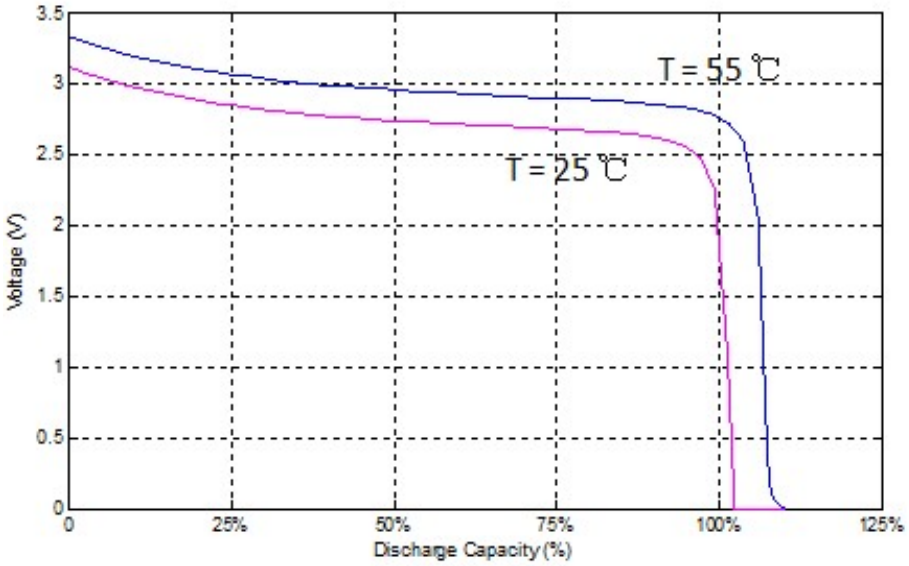

Figure 3-24 Simulated discharge curves of the battery under different temperatures

The charging and discharging curves of the battery under various number of cycles at normal temperatures

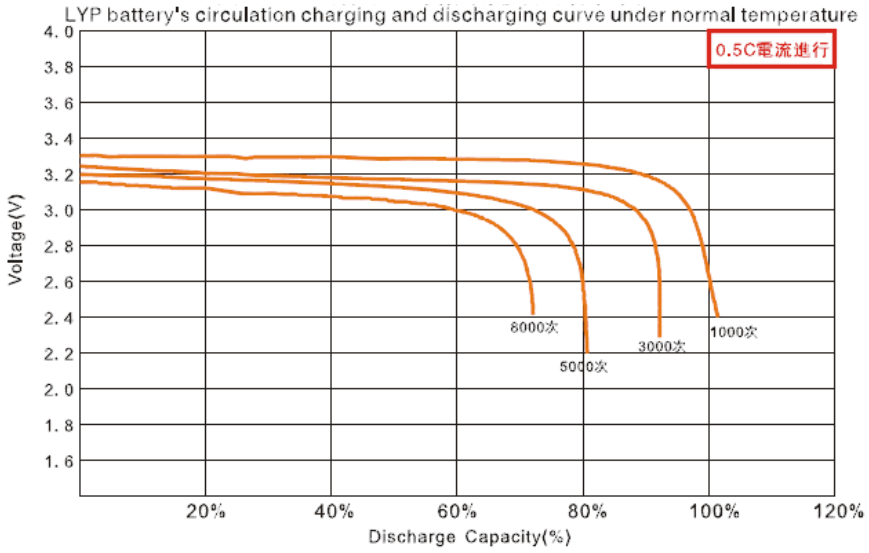

Figure 3-25 The actual discharging curves of the battery under various number of cycles

Simulated charging and discharging curves for the battery at the initial condition and after 5000 cycles under normal temperatures

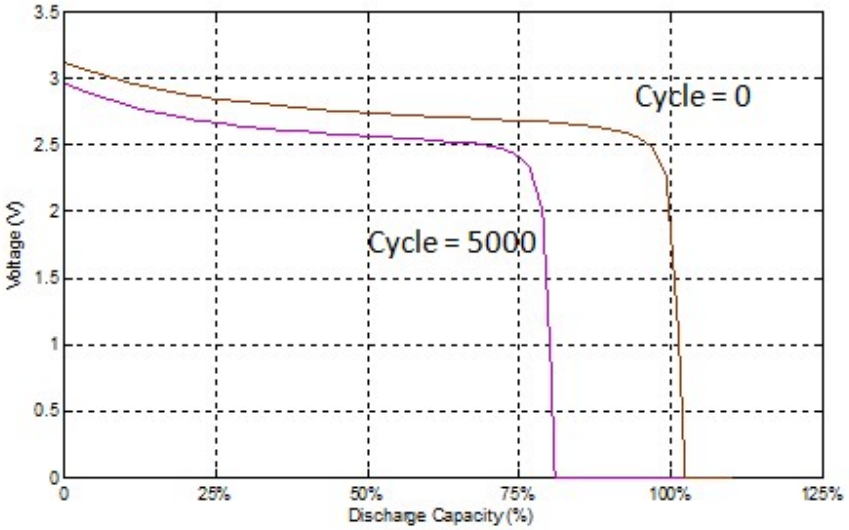

Figure 3-26 Simulated discharge curves at the initial condition and after 5000 cycles

4 BMS HARDWARE FOR ELECTRIC VEHICLES

4.1 REQUIREMENTS OF THE BMS FOR ELECTRIC VEHICLES

For small applications using lithium-ion batteries, such as laptop computers, the BMS design could be as simple as an application-specific integrated circuit (ASIC) that provides complete BMS functions.

For large lithium-ion battery packs, there are two limitations to these chips. The first limitation is that these chips are designed for low battery currents usually sensed by a PCB-mounted resistor and not for the high currents typically present in large packs sensed using a Hall-effect sensor or a current shunt. Any powerful intelligence in the chips would not be useful without knowledge of the battery current. The second limitation is that these chips could only handle several cells arranged in series. To overcome these limitations, electric vehicles should use BMSs intended for large packs instead those intended for small packs.

4.1.1 ANALOG BMS

The simpler and more common BMS designs usually use many analog BMSs. A regulator such as a Zener diode could be placed across a lithium-ion cell to bypasses part or all of the charging current when the cell is full to protect it from overcharging. However, Zener diodes have a very soft knee when the lithium-ion cells are at a low voltage. Because the cells conduct a large current, they could be quickly discharged.

Therefore, the regulators in actual designs use a generic analog IC and some form of a balancing shunt instead of a Zener diode.

In addition to protection, an analog BMS could also be used to monitor the cell voltage by sending a request to the external system to stop the battery current when the voltage of any cell is too low or too high. In the distributed topology, the BMS contains a cell circuit across each cell and a master controller. If the voltage of any cell exceeds the limit, the output of the cell circuit is reported to the master controller. For a localized BMS, all the cells in the battery pack are handled by a single circuit. The BMS selects one cell voltage at a time and analyzes that voltage using a pair of comparators.

Another important function of the BMS is to balance the cells. An analog BMS can balance the cells and protect them against high and low cell voltages. Generic ICs or ASICs could be designed as an analog balancer. A power switch could be added to a digital or analog system so that the BMS could cut off the battery current when the battery is operating outside of its safety zone.

4.1.2 DIGITAL BMS

The design of a digital BMS is similar to that of an analog BMS. Like the analog BMS, digital BMSs can be constructed with different topologies. To measure the cell voltage and temperature, a localized circuit could be used per cell. Alternatively, the circuit could be shared among various cells. The cell voltages could be simultaneously measured when one cell is used to power one device. It is very important to calculate the cell resistance

because the voltage of each cell could affect the instantaneous battery current. Thus, the voltage needs to be discretely measured. In contrast, a shared circuit is used to measure the voltages of multiple cells in a localized BMS design. This usually causes the number of components to decrease.

It is crucial for the BMS to be able to measure the battery current, the source current and the load current separately. Therefore, the BMS needs to have one or more current sensors to measure the battery current unless other devices in the system are able to report the current to the BMS. Current transformers can measure the current in AC circuits very accurately. However, BMSs are used in DC circuits; they cannot use current transformers to measure the current. Therefore, only current shunts and Hall-effect sensors can be used to measure the current in DC circuits.

In addition to current measurement, BMSs need to evaluate the state of the pack. Most digital BMSs use a software program to perform any of the following functions:

- Evaluate the cell operation within its SOA;
- Estimate the SOC and DOD;
- Calculate the resistance;
- Measure the capacity;
- Estimate the SOH.

To protect the battery by heating, cooling, or interrupting and reducing the current flow, the BMS needs to communicate with the external system. This could be achieved using dedicated wires or data links.

The final function of the BMS is to optimize the battery, which includes balancing the SOC of the battery and switching off the battery to prevent it from operating outside its SOA. Contactors, transistors or solid-state relays could all be used as switches.

4.2 TI BMS SYSTEM FUNCTIONS

4.2.1 TECHNOLOGY SELECTION

The BMS could be analog or digital depending on how the cell voltage information is processed. Nevertheless, an analog front end is required for all systems. An analog BMS uses analog circuitry, such as analog comparators, op-amps and differential circuits to process the cell voltage; a digital BMS uses digital circuitry. Depending on the system's complexity, they can also be simple or sophisticated.

In sophisticated and digital BMSs, the voltage of each individual cell, its temperature and other relevant conditions are used to analyze the state of the battery pack. For a large and professional lithium-ion battery pack, these types of analysis are required. Therefore, the BMS designed in this work used digital technology.

4.2.2 TOPOLOGY SELECTION

BMSs can be separately installed on each cell, installed altogether on a single device, or installed in an intermediate form depending on the cost, reliability, installation or maintenance requirements and measurement accuracy. BMSs are divided into the following categories according to functionality: centralized, master-slave, modular, and distributed.

The topology used in the BMS for this work was the master-slave topology, which is very similar to a modular system. In this topology, multiple identical modules (the slaves) were used to measure the voltage of certain cells. A master controller independent of the slaves is used to handle computation and communications instead of measuring the voltage.

The master-slave topology was used for this work because it had more advantages and fewer disadvantages compared with other topologies. Because each module could be placed closer to the battery, the wires to the cells were easier to manage. In addition, the system could be easily expanded to include larger packs by adding BMS slave modules. Because the system was optimized for a single task of measuring cell voltages, the cost of each slave was less than the cost of the slaves for modular topology. Nevertheless, the cost of implementing this topology was slightly higher than implementing other topologies because the slave modules may contain unnecessary functions that require extra tap wires to connect. In addition, not all inputs of the slave modules were used because of their physical locations.

4.2.3 FRONT IC SELECTION

The front IC used in the BMS system for this work was a specially designed lithium-ion battery pack protector that could be stacked in three to six cells placed in series. This chip was used as an analog front end that incorporated a precision analog-to-digital converter and a precision 5-V regulator to power the user circuitry. Furthermore, it provided independent cell voltage and temperature protection in addition to the cell balancing function.

The chip measured cell voltages with high speed and accuracy because it was integrated with a voltage translation and precision analog-to-digital converter (ADC) system. The chip provided full protection for overvoltage, undervoltage, and overtemperature conditions, and no external components need to be configured to enable the protection features. The chip set the FAULT output immediately when the safety thresholds were exceeded.

The ADC system of the chip was independent of the cell temperature, voltage measurement, and protective functions. An Error Check/Correct (ECC) OTP EPROM stored the programmable detection delay times and protection thresholds. These capabilities increased the flexibility and reliability of the BMS.

A host controller could be used with the front IC to maximize the functionality of the BMS. However, it was not necessary for the protective functions.

4.2.4 MASTER CONTROLLER SELECTION

The master controller of the BMS for this work was an ultra-low power microcontroller that belonged to a large family of products. The microcontroller consisted of several devices featuring different sets of peripherals targeted for various applications, including a powerful 16-bit RISC CPU, 16-bit registers, and constant generators that contributed to maximum code efficiency. A digitally controlled oscillator allowed the controller to wake up from the sleep mode to the active mode in less than 5 μs. Combined with extensive low power modes, the architecture was optimized for low power consumption.

The microcontroller supported USB 2.0, four 16-bit timers, a high-performance 12-bit ADC, two universal serial communication interfaces, a hardware multiplier, DMA, a real-time clock module with alarm capabilities, and 63 I/O pins in its configuration. The microcontroller was designed for applications such as analog and digital sensor systems and data loggers, which required connectivity to various USB hosts including a BMS.

4.2.5 LIMITATIONS OF THE TI BMS

The drawbacks of the BMS designed by TI are listed below:

1. There is no SOC estimation.
2. There is no current measurement.
3. There is no user interface.
4. There is no temperature measurement.

5. There is no cooling system.

4.3 IMPROVEMENT OF THE TI BMS

4.3.1 USER INTERFACE

The user interface represents everything that is designed into an information device with which a human being may interact, which includes the display screen, keyboard, mouse and light pen. It helps people communicate with machines, computers or other equipment. The user interface can also be called the “total user experience,” which may include the content that is presented to the user within the context of the user interface.

The cell voltage, current, SOC and temperature are all critical to the end-user and should be shown in the user interface. To achieve this goal, an LCD screen is used to display all the useful information to the user. The microcontroller controlled the LCD by the computer programming language C.

The LCD control chip was a 262,144-color, one-chip SoC driver for a-TFT liquid crystal display with a resolution of 240 (RGB) × 320 dots comprised of a 720-channel source driver, a 320-channel gate driver, 172,800 bytes of RAM for the graphic data of 240 (RGB) × 320 dots, and a power supply circuit. The chip was an ideal LCD driver for medium or small size portable products, such as digital cellular phones, smart phones,

PDAs and PMPs where long battery life is a major concern. Therefore, the chip was suitable for BMS applications.

4.3.2 THERMAL MANAGEMENT

Temperature monitoring and control

Because the cells must remain in the SOA at all times, temperature detection is one of the most common tasks for a BMS. The BMS design for this work included a temperature sensor.

The sensor consisted of a digital thermometer that provided 9 to 12-bit Celsius temperature measurements with an alarm function and nonvolatile user-programmable upper and lower trigger points. The sensor communicated with a central microprocessor over a 1-wire bus that required only one data line and ground. It had an operating temperature range of - 55 °C to + 125 °C and was accurate to ± 0.5 °C over the range of -10 °C to + 85 °C. In addition, the sensor could derive power directly from the data line, eliminating the need for an external power supply.

Cooling system

A fan system controlled by pulse-width modulation (PWM) based on the temperature measured by the sensor was used for cooling in the BMS for this work.

PWM is a common method to control fans. For example, modern computer motherboards with multi-core CPUs are cooled with PWM controls.

Unlike the linear methods that are based on voltage drops, PWM switches the input voltage between fully on and fully off at a current with a specific frequency. The ratio between the "on" time and "off" time is called the duty ratio. By controlling the duty ratio, the fan can be driven at different rotation speeds.

The PWM input was delivered to the fan through the control signal pin. The fan speed response to this signal should be a continuous and monotonic function of the duty cycle of the signal, from 100% to the minimum specified RPM. The fan RPM should match the PWM duty cycle within ± 10%. If no control signal was present, the fan operated at the maximum RPM.

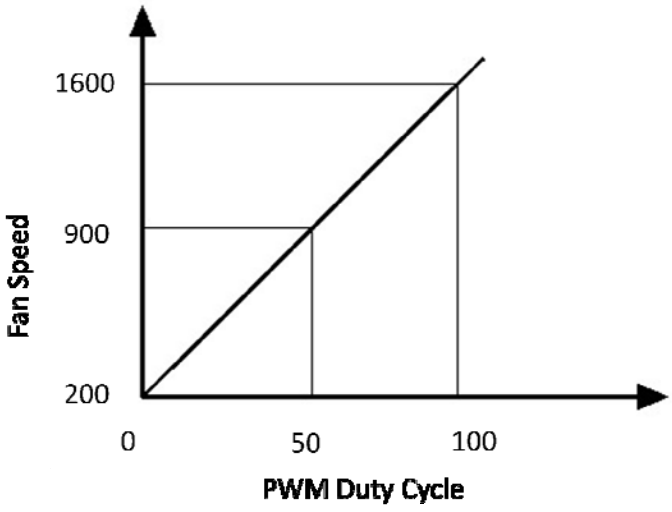

Figure 4-1 Fan speed response to the input signal from the PWM control

4.3.3 CURRENT MONITORING

Current is one of the most important parameters in the operation of a battery pack. To maintain the battery cell within its SOA during charging and discharging, the current was measured by a current sensor.

The current sensor was a Hall-effect sensor. The Hall effect is the production of a voltage difference across an electrical conductor that is transverse to an electric current in the conductor and a magnetic field perpendicular to the current. It was discovered by Edwin Hall in 1879. By sensing the current provided to a load and using the voltage applied to a device as the sensor voltage, it is possible to determine the power dissipated by a device.

Compared with other sensors, the Hall-effect sensor is easy to mount and small in size. It only requires one design for a wide range of current ratings and highly resistant to external interference.

4.4 BMS SYSTEM

The BMS design for this work was based on an original TI BMS. A microcontroller and three front ICs were used and a standard evaluation board was used for each of the two chips. A current module, a temperature module, a cooling module and a display module were added to the design so that the BMS would have all of the required functions.

4.4.1 BMS HARDWARE CONFIGURATION

Standard wire jumpers were used to connect the two evaluation boards. The microcontroller board and the isolation circuitry on the front IC board could be powered using the USB port on the host computer or an external power supply.

The block diagram of the entire system is shown below:

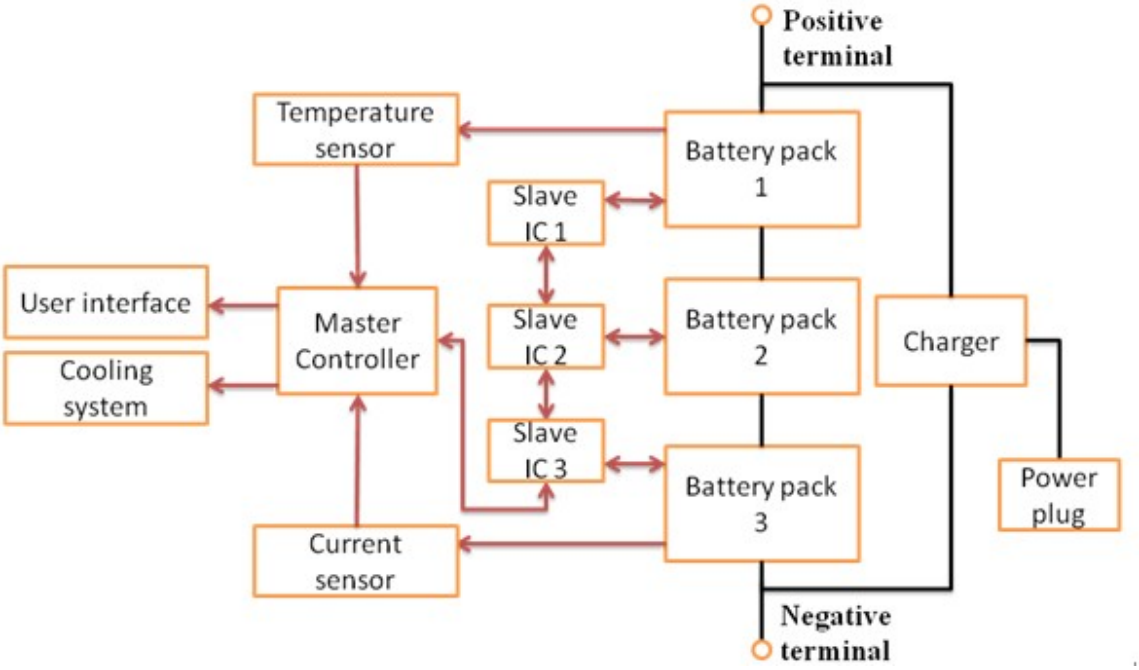

Figure 4-2 BMS system block diagram

After the master controller board and the front IC board were connected, four additional modules were connected. The LCD display board was powered by a 5-V DC and connected to the master controller board through standard wires. The temperature module was connected via the temperature sensor mounted on this board to measure the temperature of the battery pack. Three small LED lights were used to indicate the temperatures: the green, yellow and red lights indicated low, medium and high temperatures, respectively.

The cooling module was also connected to the microcontroller board. The fan on the cooling module was controlled by the master controller based on the temperature reading from the sensor, and the fan operated in three speed ranges according to the temperature ranges. The last module connected was the current module. The Hall-effect sensor was mounted on the cable connecting the battery packs. Both the discharging current and the charging current could be read and sent to the master controller.

4.4.2 BMS SOFTWARE FLOWCHART

The software to operate the BMS was programmed to configure, monitor and control multiple daisy-chained front IC devices. These daisy-chained devices monitored a battery pack that included 18 cells. The software had the following tasks:

- Configure the multi-stacked battery pack;
- Monitor the voltage and temperature of the multi-cell battery pack;
- Monitor the individual cell voltage;
- Monitor the battery pack current;
- Balance the passive cell;
- Protect against cell overvoltage and undervoltage;
- Protect against over-temperature;
- Detect the charge and discharge mode;
- Communicate to a host device using USB or UART;
- Display all information on the LCD screen;

• Control cooling fan speed based on temperature.

The first task of the battery management software was to initialize the peripherals controlled by the microcontroller. The next task was to build the battery stack by detecting and configuring the front ICs. Then, the software identified the status of the cells and the battery pack by reading the voltages, current and temperatures.

By sampling the cell voltages and the integrity of the battery pack every second, the battery management software continuously checked the battery pack for a “FAIL” condition. If there were no corrective actions necessary or any pending tasks, the system went to low power mode. The figure below shows the flowchart of the software and provides a brief description of this process.

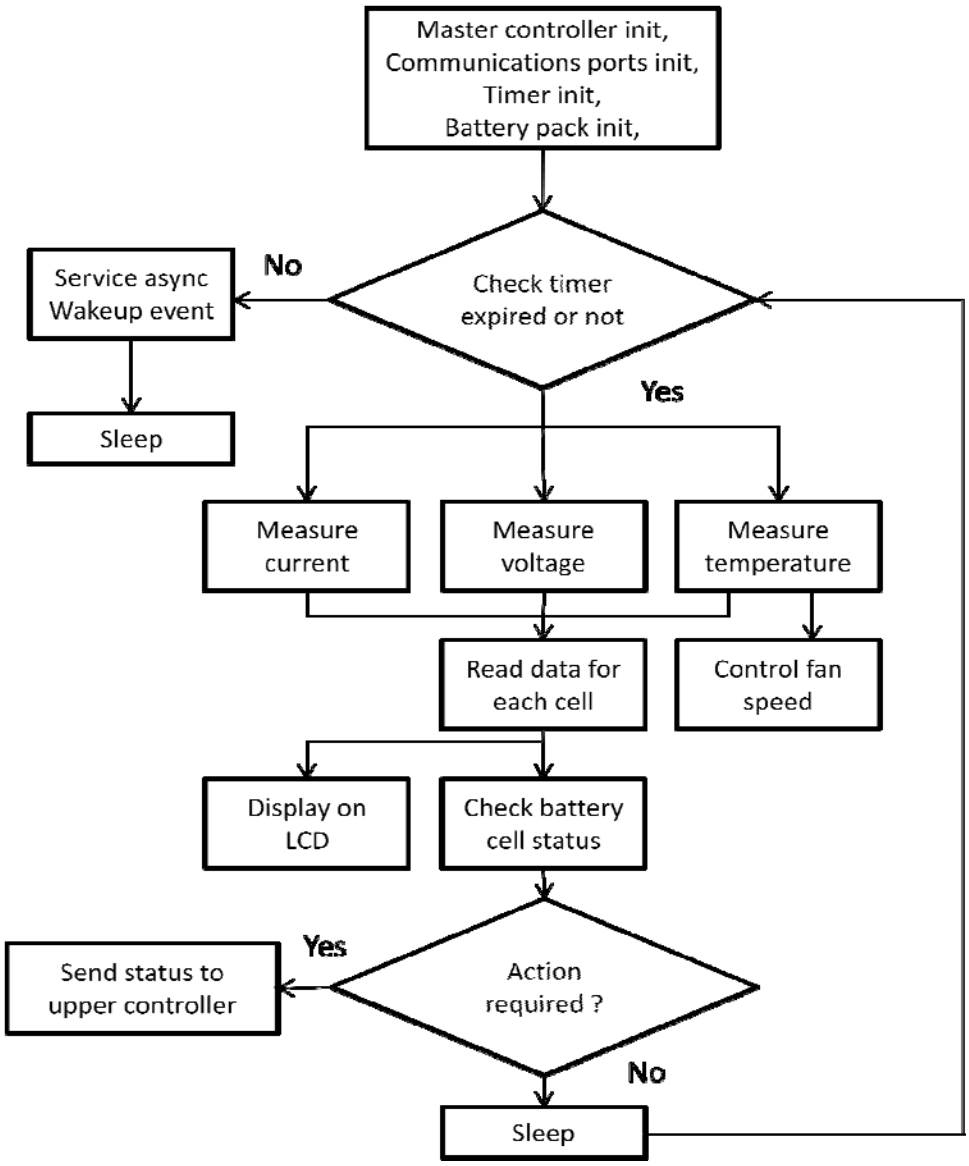

Figure 4-3 Battery management software flowchart

The BMS software protected the battery pack and the cells from undesired operating conditions by comparing the predefined values stored in flash memory with the actual values at runtime. The threshold values were defined based on the lithium-ion cell characteristics provided by the datasheet. The threshold values of the battery pack were defined according to the threshold values of the cells.

The most common manifestation of imbalance was a difference in the cell voltages, which could be corrected by gradually bypassing the cells with higher voltages. Based on the differences between the cell voltages, a passive cell-balancing method was implemented in this BMS. Bypass was activated when the cell voltage difference exceeded the predefined threshold in the charging mode.

The software determined the cells to bypass based on the voltage difference between the cell with the highest voltage in the entire pack and the other cells. After the cells were bypassed, the software performed multi-cell balancing simultaneously.

4.5 EXPERIMENTAL RESULTS AND DISCUSSION

The battery cell used in the experiment was the Thundersky LYP-40Ah. The parameters of this battery cell are shown in the table below.

Table 4-1 LYP-40Ah battery cell parameters

Battery Model	WB-LYP40AHA	
Nominal Capacity	40 Ah	
Operation Voltage	Charging	4.0 V
	Discharging	2.8 V
Maximum Charge Current	3 CA	

Maximum Discharge Current	Constant Current	3 CA
	Impulse Current	20 CA
Standard Charging/Discharging Current	0.5 CA	
Operating Temperature	Charge	- 45 to 85℃
	Discharge	- 45 to 85℃
Weight	1.5 kg +/- 50 g	

In order to compare with experimental results, relative simulation cases were done. The parameters of battery model used in simulation cases are: E_0 = 59.5252, $R_{internal}$ = 0.029255, K = 0.53438, A = 7.41, B = 2.0833.

The first experiment was to fully discharge the battery pack because the battery pack was fully charged at approximately 65 V. An electric motor was used to simulate electrical load. The load resistance was set to 9 Ω. The load was assumed to remain constant during the entire discharging process, which lasted approximately 7 hours.

The current curves are shown below. Figure 4-4 shows the original experimental discharging current data. The sampling time was 1 second, and the fluctuation of the curve was high due to the accuracy of the current sensor.

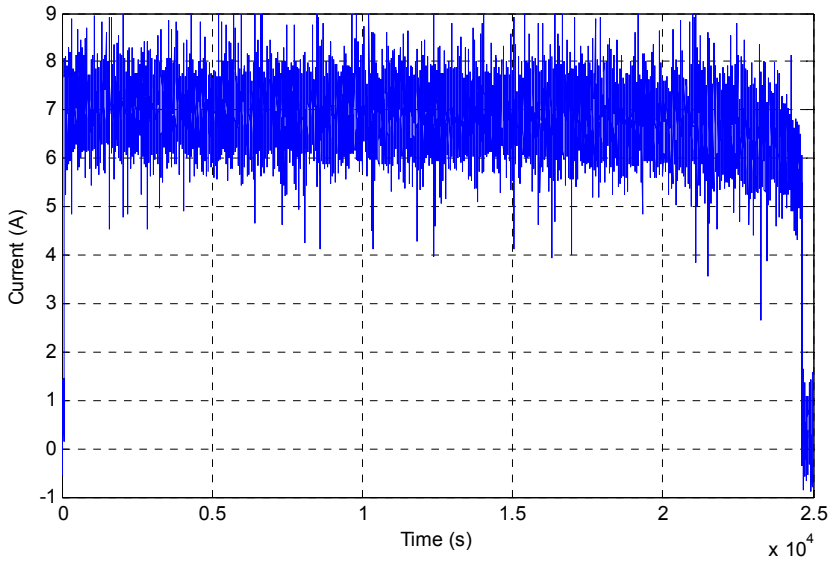

Figure 4-4 Experimental discharging current curve (1s)

Figure 4-5 was obtained by taking the average of the experimental data every 10 seconds; this figure showed less data fluctuation compared to the previous figure.

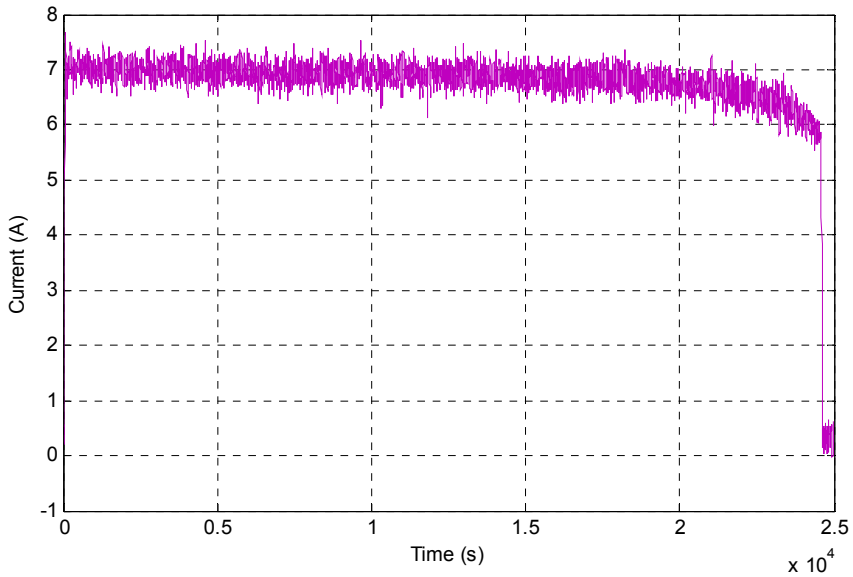

Figure 4-5 Experimental discharging current curve (10 s)

Figure 4-6, which shows almost no fluctuation in the curve, was obtained by taking the average of the experimental data every 100 seconds.

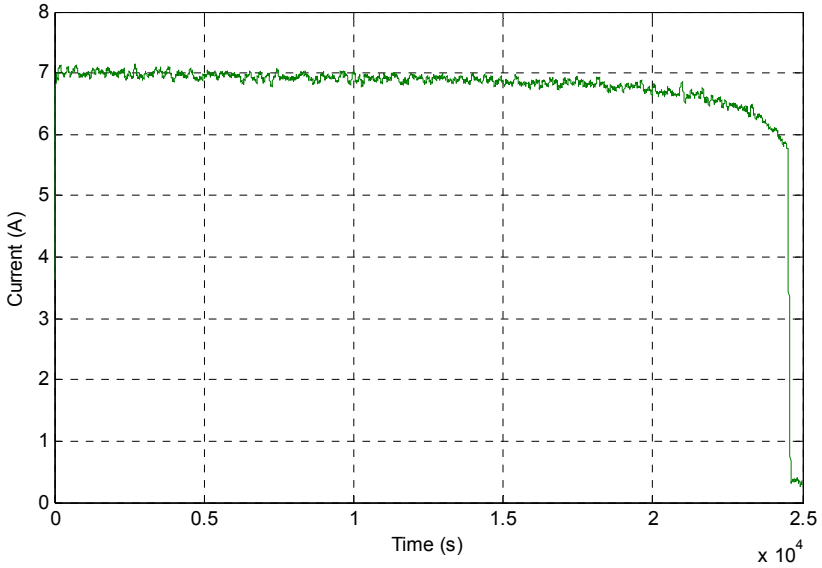

Figure 4-6 Experimental discharging current curve (100 s)

A simulation was conducted based on the same type of battery and experimental setup, and the result of the discharging current curve is shown in Figure 4-7.

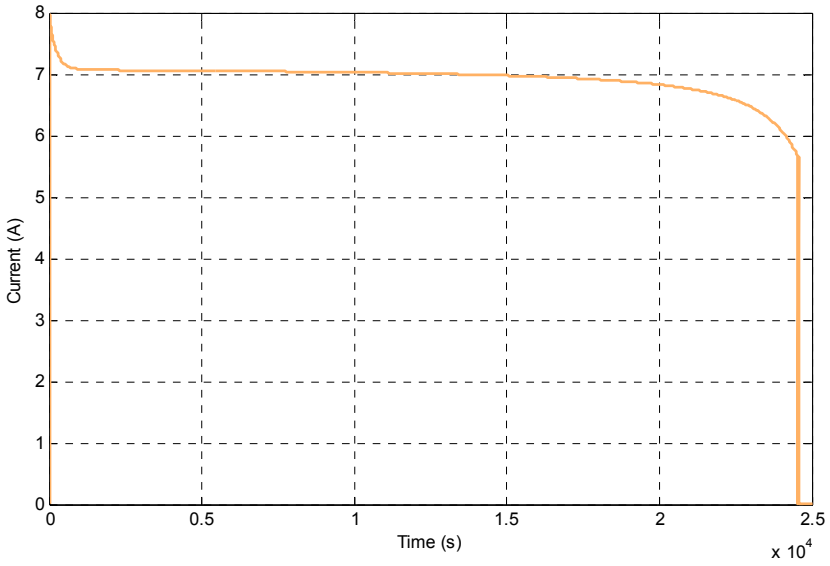

Figure 4-7 Simulated discharging current curve

Figure 4-8 shows the experimental and simulated results in the same figure, and both curves were similar in shape.

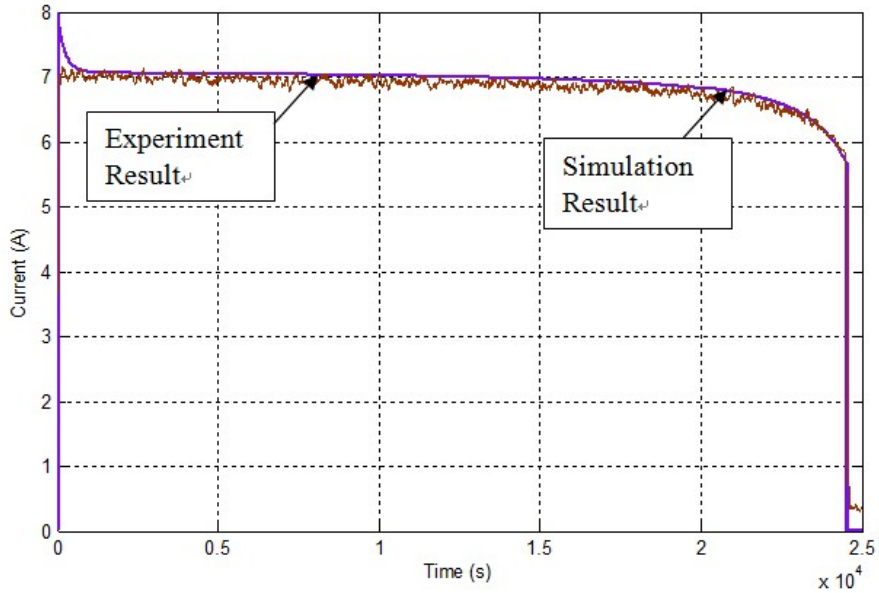

Figure 4-8 Experimental and simulated discharging current curves

The experimental discharging voltage curve is shown in Figure 4-9.

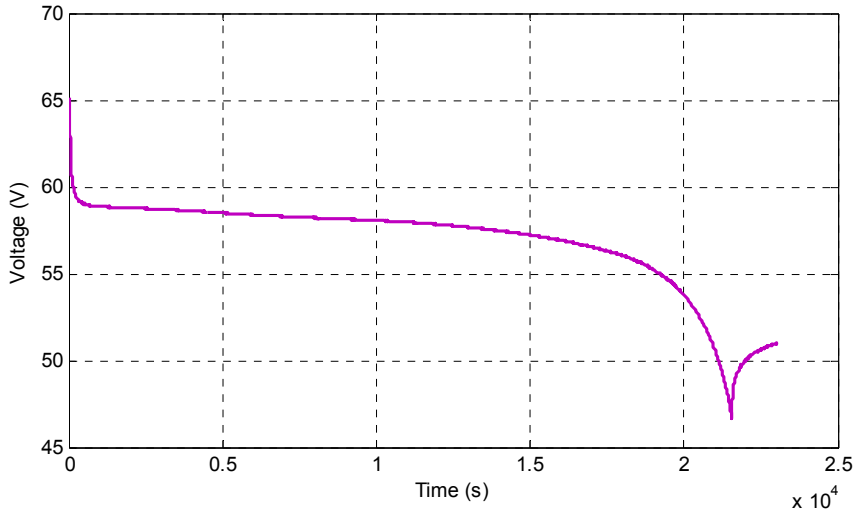

Figure 4-9 Experimental discharging voltage curve

Similarly, the simulated discharging voltage curve is shown in Figure 4-10.

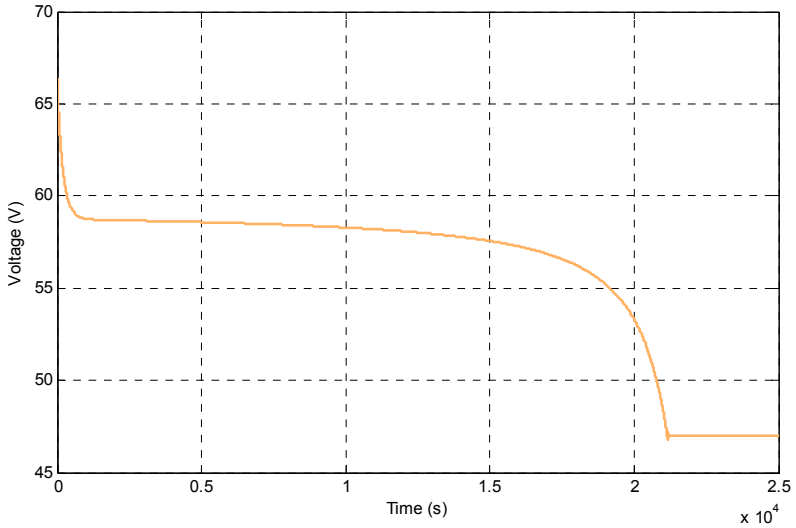

Figure 4-10 Simulated discharging voltage curve

Figure 4-11 combines the results from Figures 4-9 and 4-10. It could be seen that the experimental and the simulated curves were similar in shape. However, the simulated result did not show the voltage increase near the end of the experiment; this was the drawback of this battery model.

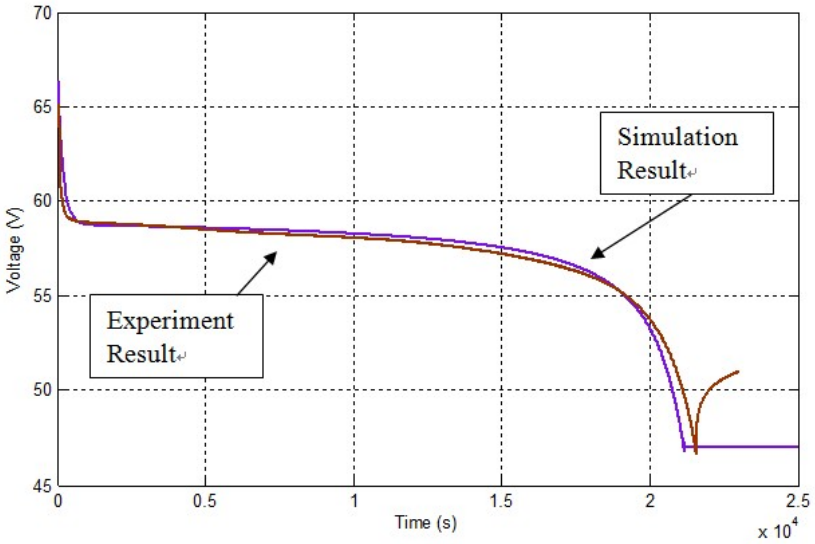

Figure 4-11 Experimental and simulated discharging voltage curves

The second experiment was to fully charge the battery pack. A CC/CV charger was used to charge the battery. The constant current was set to 15 A, and the constant voltage was set to 68.4 V. This charger could charge 18 cells at once. The entire charging process was approximately 4.5 hours.

The original data for the experimental charging current curve is shown in Figure 4-12. The negative values referred to the charging current that flowed into the battery pack.

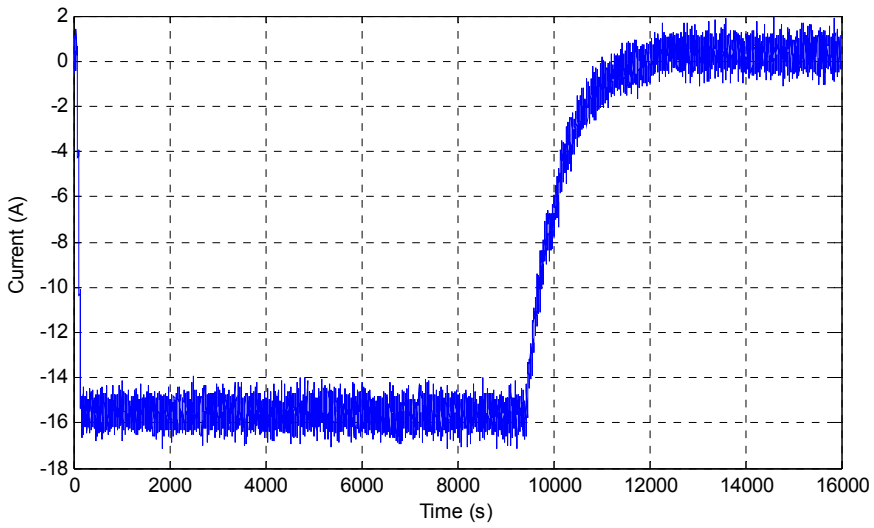

Figure 4-12 Experimental charging current curve (1s)

Figure 4-13 was obtained by averaging the experimental data every 10 seconds. The data fluctuation was lower than that observed in the previous figure.

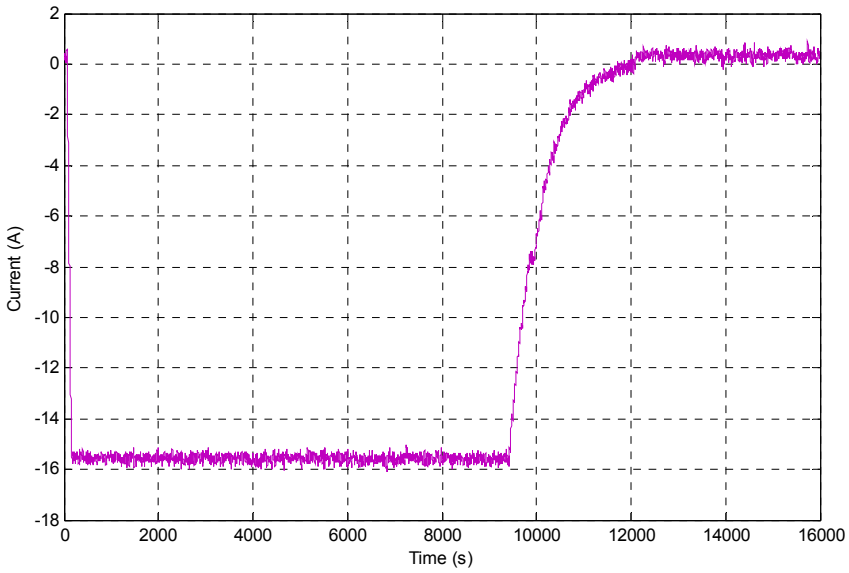

Figure 4-13 Experimental charging current curve (10 s)

Figure 4-14 was obtained by averaging the experimental data every 100 seconds; there was almost no fluctuation in this curve.

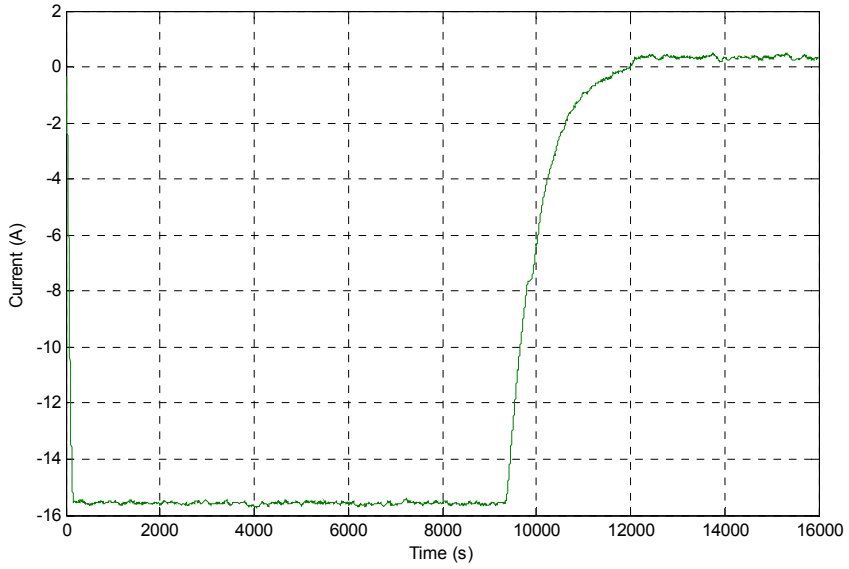

Figure 4-14 Experimental charging current curve (100 s)

A simulation was conducted based on the same type of battery and experimental setup, and the result of the charging current curve is shown in Figure 4-15.

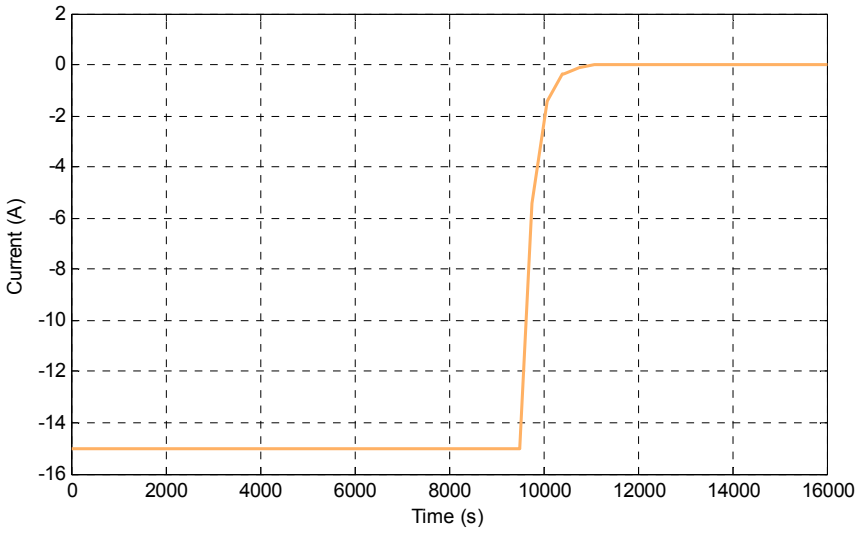

Figure 4-15 Simulation charging current curve

Figure 4-16 combines the results from Figures 4-14 and 4-15. The experimental and the simulated curves were similar in shape.

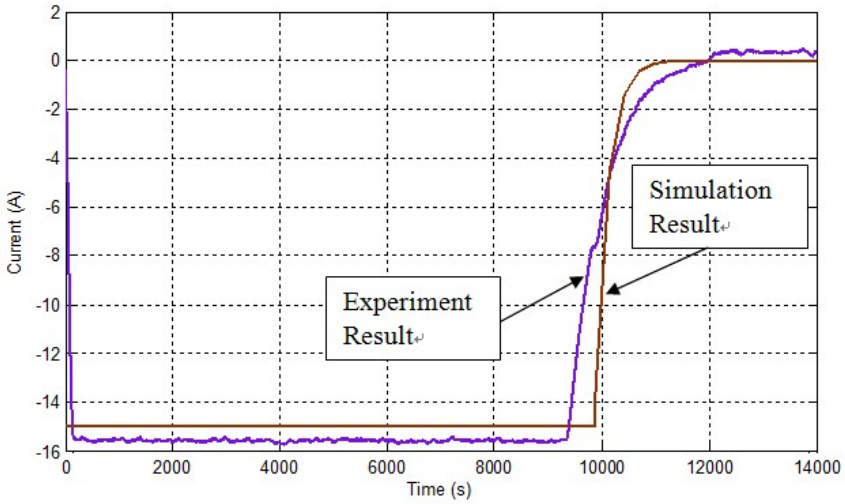

Figure 4-16 Experimental and simulated charging current curves

The experimental charging voltage curve is shown in Figure 4-17.

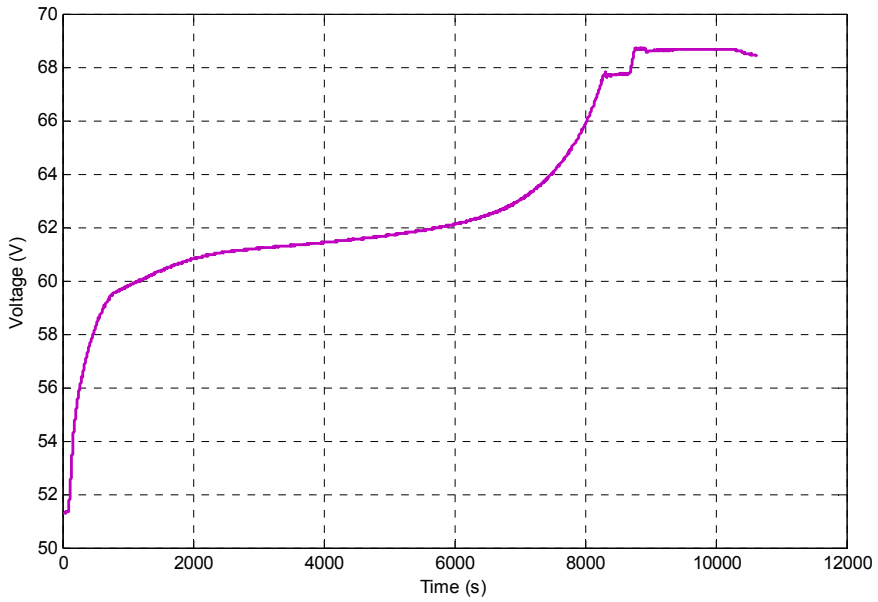

Figure 4-17 Experimental charging voltage curve

Similarly, the simulated charging voltage curve is shown in Figure 4-18.

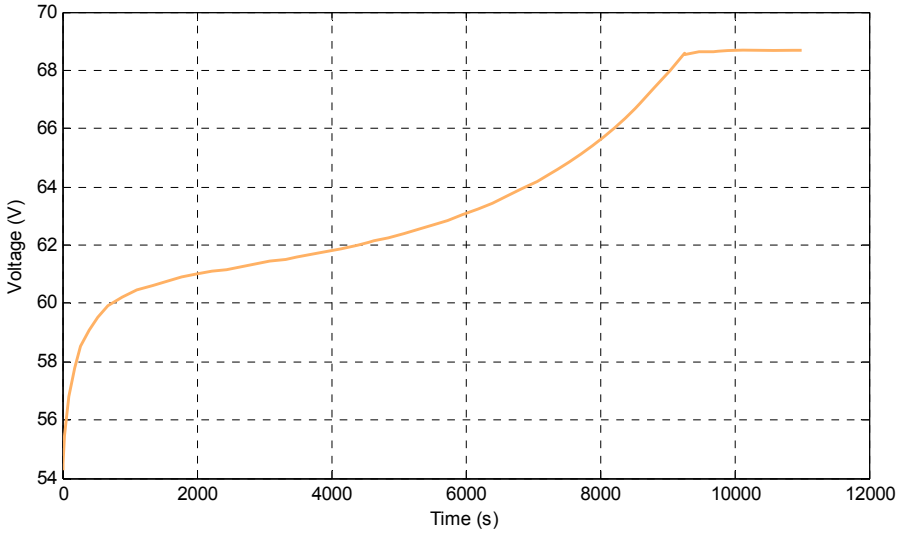

Figure 4-18 Simulated charging voltage curve

Figure 4-19 shows the results from Figures 4-17 and 4-18 in the same figure. It could be seen that the experimental and the simulated curves were similar in shape.

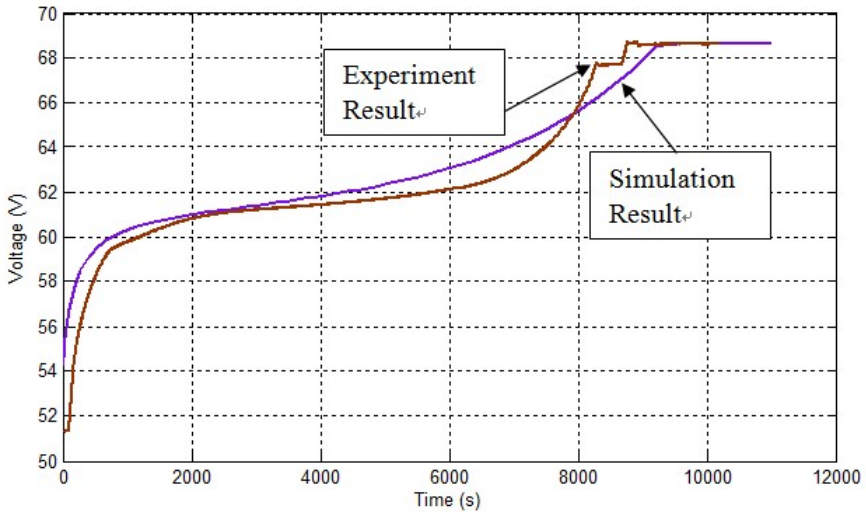

Figure 4-19 Experimental and simulated charging voltage curves

If the charger was connected to the battery pack after the battery was fully charged, the voltage dropped as time increased (as shown in Figure 4-20).

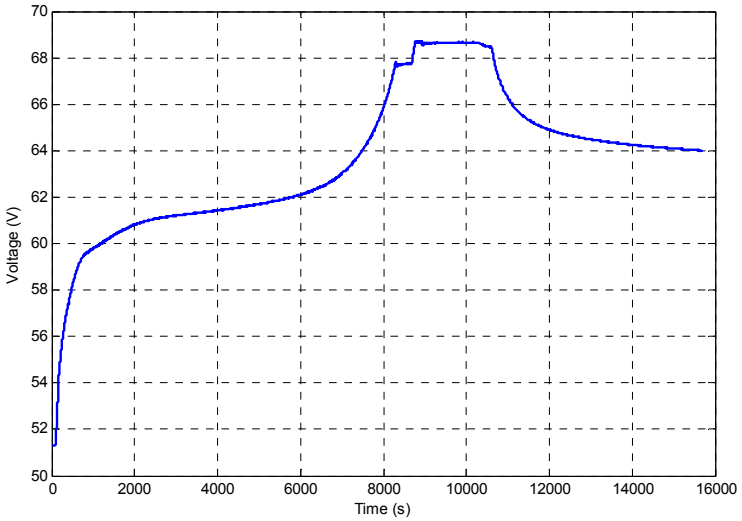

Figure 4-20 Experimental charging voltage curve (charger effect)

The voltage drop was attributed to the physical connection between the battery pack and charger. Although the charger automatically turned off at the end of the charging process, it became a load for the battery pack and caused the battery voltage to drop.

The same phenomenon was observed in the simulation, as shown in Figure 4-21.

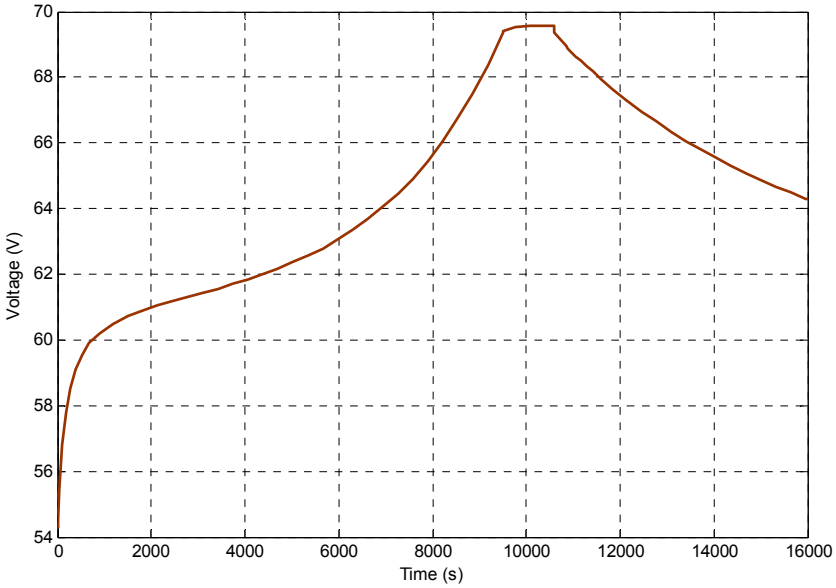

Figure 4-21 Simulated charging voltage curve (charger effect)

The final experiment was cell balancing. Six of the cells in the battery pack were monitored for this experiment. The 6 cells were initially unbalanced. However, cells with higher voltages discharged themselves over time until all the cells were balanced. The experimental voltage curves of these 6 battery cells are shown in Figure 4-22.

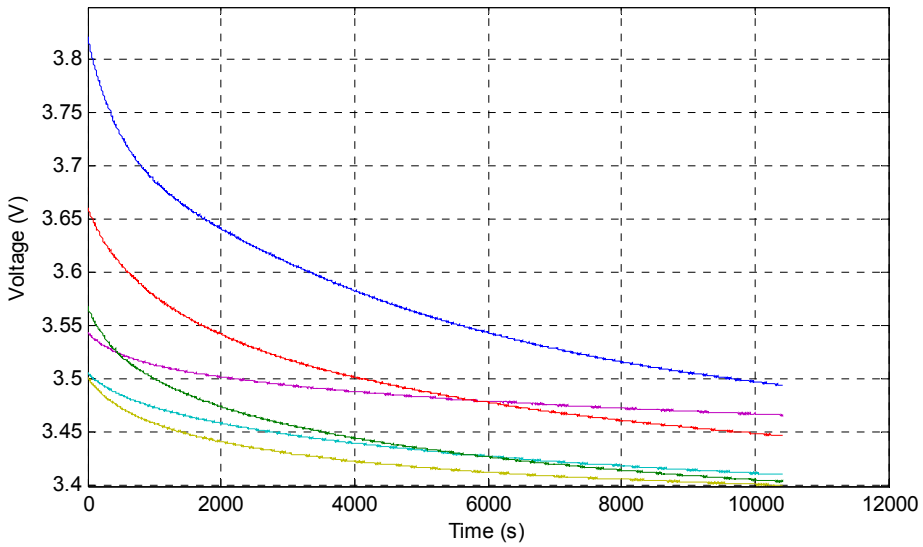

Figure 4-22 Experimental cell-balancing curves

A simulation of the cell balancing experiment over the same length of time produced similar results, as shown in Figure 4-23.

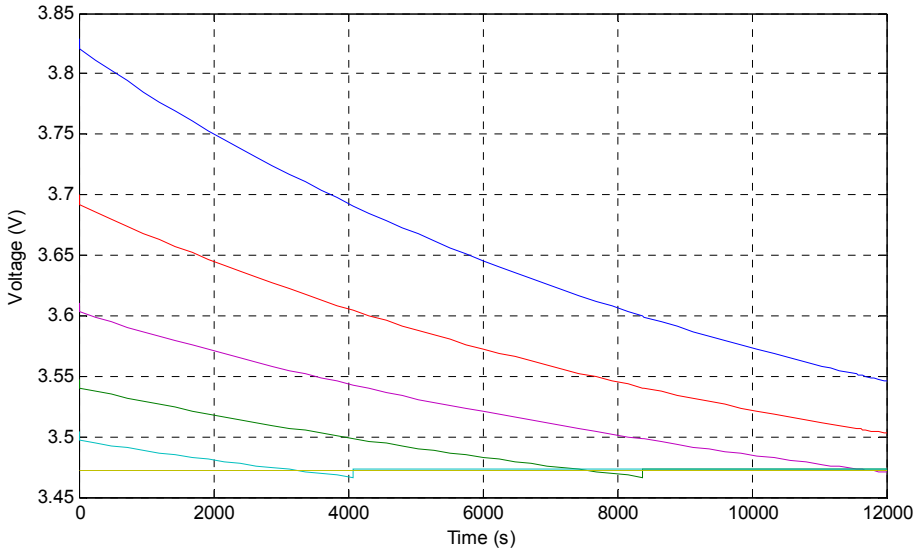

Figure 4-23 Simulated cell-balancing curves (12000 s)

Due to the limitation of the experiment, the experiment only lasted 12,000 seconds. However, the cell was not balanced at 12,000 seconds. The simulation results in Figure 4-24 shows the voltage curves in the balanced state.

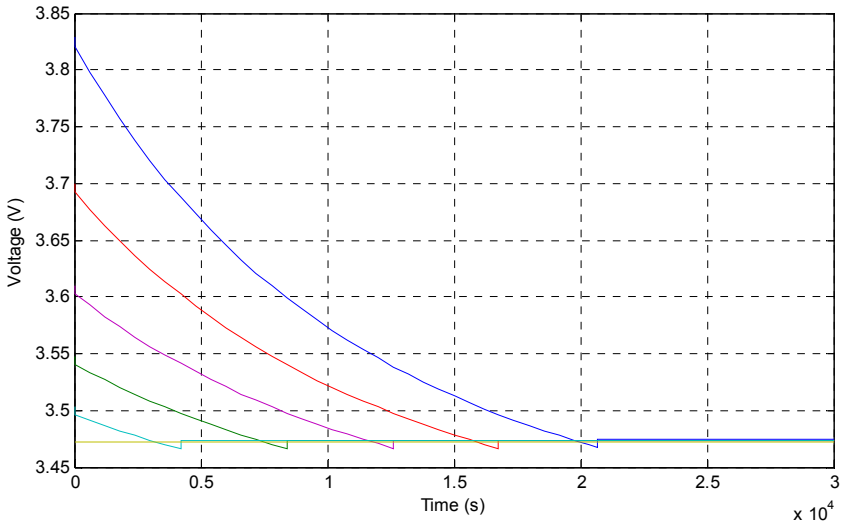

Figure 4-24 Simulated cell-balancing curves (30000 s)

The results above indicated that all experimental data matched simulation results and that the BMS hardware system operated adequately.

5 CONCLUSIONS AND RECOMMENDATIONS

5.1 CONCLUSIONS

This work first introduced the background of electric vehicles, lithium-ion batteries and the BMS. The details of the BMS, including its definition, objectives, functions and topologies were then discussed. The literature on battery modeling and BMS hardware system design were reviewed in the following section. The limitations of early battery models and the disadvantages of other BMS hardware systems were also reviewed. The objectives and outline of this thesis were then presented.

An improved battery model was proposed in this work by considering the self-discharging effect, the temperature effect and the fading-capacity effect observed in all batteries. The model was simulated using Matlab/Simulink, and the simulation results were discussed. A novel BMS hardware system based on the design of a TI BMS was introduced. It improved the original system by adding a user interface, a thermal management system and a current-monitoring function. The experimental results of this improved system were subsequently discussed. Finally, the results from a simulation based on an actual Thundersky battery were compared with the results from the experiments on the BMS hardware system.

5.2 FUTURE WORK AND RECOMMENDATIONS

Many battery models do not simulate of the discharging behavior of actual batteries. When batteries are nearly fully discharged, and the load is removed from the battery, the voltage of the battery will increase; when the load is connected to the battery, and the current resumes, the voltage of the battery will drop to the nominal value. Such discharging behavior should be simulated in future battery models. In addition, the performance of battery models could be further improved.

To improve BMS hardware systems, a method could be created to allow the BMS to communicate with vehicle controllers and other sub-systems in the vehicle, such as the motor controller. In addition, a protection device could be added to the system to switch off the battery pack when it operates out of its SOA. Furthermore, the cell-balancing function could be improved. A BMS could then be developed for use in electric vehicles.

REFERENCES

[1] Sandeep Dhameja, Electric Vehicle Battery Systems, 2002, ISBN 0-7506-9916-7

[2] Elithion website, http://liionbms.com/php/index.php

[3] H.J. Bergveld, Battery Management Systems Design by Modeling, 2001, ISBN 90-74445-51-9

[4] Shepherd, C. M., Design of Primary and Secondary Cells - Part 2. An equation describing battery discharge, Journal of Electrochemical Society, Volume 112, July 1965, pp 657-664.

[5] Olivier Tremblay, Louis-A. Dessaint, Experimental Validation of a Battery Dynamic Model for EV Applications, World Electric Vehicle Journal Vol. 3 - ISSN 2032-6653

[6] D. Fisher, A. Lohner, and P. Mauracher, “Battery management: Increase in the reliability of UPS,” ETZ, vol. 117, pp. 18–22, 1996.

[7] Z. Noworolski and J. M. Noworolski, “A microcomputer-based UPS battery management system,” in Proc. IEEE APEC’91, 1991, pp. 475–479.

[8] K. Shimitzu, N. Shirai, and M. Nihei, “On-board battery management system with SOC indicator,” in Proc. Int. Electric Vehicle Symp., vol. 2, 1996, pp. 99–104.

[9] J. Alzieu, P. Gangol, and H. Smimite, “Development of an on-board charge and discharge management system for electric-vehicle batteries,” J. Power Sources, vol. 53, pp. 327–333, 1995.

[10] D. Bell, “A battery management system,” Master’s thesis, School Eng., Univ. Queensland, St. Lucia, Australia, 2000.

[11] J. M. Andrews and R. H. Johnes, “A VRLA battery management system,” in Proc. INTELEC, 1996, pp. 507–513.

[12] W. Retzlaff, “On board battery diagnostic and charge equalizing system (BADICHEQ),” in Proc. 11th Int. Electric Vehicle Symp., vol. 2, Sept. 1992, pp. 20.03/1–20.03/12.

[13] N. Kutkut, D. Divan, and D. Novotny, “Charge equalization for series connected battery strings,” IEEE Trans. Ind. Applicat., vol. 31, pp. 562–568, May/June 1995.

[14] N. Kutkut, H. Wiegman, D. Divan, and D. Novotny, “Equalization of an electric vehicle battery system,” IEEE Trans. Aerosp. Electron. Syst., vol. 34, pp. 235–246, Jan. 1998.

[15] N. Kutkut, D. Divan, and D. Novotny, “Design considerations for charge equalization on an electric vehicle battery system,” IEEE Trans. Ind. Applicat., vol. 35, pp. 28–35, Jan./Feb. 1999.

[16] Minxin Zheng, Bojin Qi, Hongjie Wu, A Li-ion Battery Management System Based on CAN-bus for Electric Vehicle, 2008, IEEE

[17] John Chatzakis, Kostas Kalaitzakis, Nicholas C. Voulgaris, and Stefanos N. Manias, Designing a New Generalized Battery Management System, 2003, IEEE

[18] Zhang Haoming, Sun Yukun, Ding Shenping, Wang Yinghai, Full-digital Lithium Battery Protection and Charging System Based on DSP, 2008, Proceedings of the 27th Chinese Control Conference

[19] Texas Instruments, www.ti.com, December 2010

VITA AUCTORIS

NAME: Rui Hu

PLACE OF BIRTH: Nanjing, Jiangsu, China

YEAR OF BIRTH: 1982

EDUCATION: Nanjing University of Aeronautics and Astronautics, Nanjing, Jiangsu, China
2000 – 2004 B.Eng.

University of Windsor, Windsor, Ontario, Canada
2008 – 2009 MEng

University of Windsor, Windsor, Ontario, Canada
2009 – 2011 MASc